SAN FRANCISCO ESTUARY & WATERSHED SCIENCE
Sponsored by the Delta Stewardship Council and UC Davis Institute of the Environment

RESEARCH

Managed Wetlands for Climate Action: Potential Greenhouse Gas and Subsidence Mitigation in the Sacramento–San Joaquin Delta

Lydia J. S. Vaughn[1], Steven J. Deverel[2], Stephanie Panlasigui[1], Judith Z. Drexler[3], Marc A. Olds[2], José T. Díaz[2], Kendall F. Harris[1], James Morris[4], J. Letitia Grenier[1,5], April H. Robinson[1], Donna A. Ball[1]

ABSTRACT

In the Sacramento–San Joaquin Delta (Delta), widespread drainage of historical wetlands has led to extensive subsidence and peat carbon losses, as well as high ongoing greenhouse gas (GHG) emissions. Large-scale wetland restoration and conversion to rice fields has the potential to mitigate these effects while conferring flood protection and creating habitat for wetland species. To explore the scale of these potential benefits, this study evaluated the effects of seven Delta-wide land-use scenarios on carbon stocks, land-surface elevation, GHG emissions, and habitat. Peat mapping and data from peat cores indicate that soil carbon stocks have decreased between the early 1800s and 2010s from 288 ± 15 to 145 ± 14 million metric tons (megatonnes; Mt) of carbon (C). If existing land uses continue, the Delta could lose an additional 8.3 Mt C during the coming 40 years, equal to average GHG emissions of 1.2 Mt CO_2 equivalents (CO_2e) yr^{-1}. Future restoration and rice-farming scenarios indicate that wetland restoration could theoretically halt GHG emissions, converting the Delta from a large GHG source to a weak net source or sink. Across three future scenarios based on existing restoration targets, wetland creation and conversion to rice fields reduced GHG emissions by 0.39 to 0.67 Mt CO_2e yr^{-1}, with per-area benefits of 16 to 28 metric tons (tonnes; t) CO_2e per hectare (ha) yr^{-1}. Differences among scenarios in extents of wetland types influenced their relative benefits for different management goals. Tidal restoration and conversion to rice fields enhanced habitat benefits and offered a source of agricultural income, but with reduced GHG mitigation compared with conversion to peat-building wetlands. This highlights the importance of clear objectives when developing land-use plans. A strategic land-management portfolio that includes rice fields and both impounded and tidal wetlands could be designed to provide GHG and subsidence mitigation while offering a diverse suite of benefits for ecosystems and people.

SFEWS Volume 22 | Issue 2 | Article 3
https://doi.org/10.15447/sfews.2024v22iss4

* Corresponding author: lydiav@sfei.org
1 San Francisco Estuary Institute–Aquatic Science Center
Richmond, CA 94804 USA
2 HydroFocus, Inc.
Davis, CA 95618 USA
3 California Water Science Center
US Geological Survey
Sacramento, CA 95819 USA
4 University of South Carolina
Columbia, SC 29208 USA
5 Current: Public Policy Institute of California
San Francisco, CA 94111 USA

KEY WORDS

subsidence, soil carbon, climate change mitigation, greenhouse gas (GHG) emissions, greenhouse gas (GHG) emissions reductions, carbon dioxide removal, wetland, peat loss, restoration, multi-benefit planning

INTRODUCTION

The Sacramento–San Joaquin Delta of California (Delta) was once the largest estuarine wetland along the west coast of the US and originally consisted of 2,300 km^2 of tidal freshwater wetlands, channels, and riparian corridors (Whipple et al. 2012). In the late 1800s and early 1900s, approximately 98% of this tidal region was drained for agriculture. By the 1930s, extensive levee-building had transformed the Delta into its current configuration of more than 100 islands and tracts surrounded by 2,250 km of human-made levees and 1,130 km of waterways (Prokopovich 1985; Ingebritsen et al. 2000). Drainage of the highly organic peat soils resulted in large-scale conversion of the ~6,700-year-old carbon sink to carbon dioxide (CO_2) source, and caused widespread land-surface subsidence (hereafter, subsidence) ranging from 1 m to over 8 m in depth (Drexler, de Fontaine, and Deverel 2009; Deverel and Leighton 2010; Deverel, Ingrum, et al. 2016b).

Land-use conversion in the Delta has had consequences for local ecosystems, regional flood risk, and California's greenhouse gas (GHG) budget. Previous estimates of peat carbon stocks in the Delta suggest that roughly half the historical peat carbon stock has been oxidized to CO_2 (Drexler et al. 2019). Ongoing high GHG emissions from drained Delta soils (Hatala et al. 2012; Hemes et al. 2019) have been estimated to account for 21% of California's annual agricultural emissions (Deverel et al. 2020), and the state has identified oxidative subsidence in the Delta as a source of GHG emissions that conflict with California's carbon neutrality goal (AB 1279, Muratsuchi). In addition to subsidence and peat carbon oxidation, widespread losses of tidal marsh ecosystems and the collapse of the detritus-based food web have led to a precipitous decline in several pelagic fishes, including the Delta Smelt (*Hypomesus transpacificus*; Sommer et al. 2007; Durand 2015). Concomitant with these effects are other losses of ecosystem services that tidal marshes typically provide, such as shoreline protection from flooding (Narayan et al. 2017; Beagle et al. 2019), water-quality benefits (Knox et al. 2008; Shapiro et al. 2010), cultural services (Rouleau et al. 2021), and habitat support for a range of native flora and fauna (Perry et al. 2010; Dybala et al. 2020).

Subsidence on Delta islands also presents challenges for infrastructure and existing land uses. Eighty-seven Delta levee failures have occurred since 1950, and about one billion dollars of state funds have been invested in Delta levee maintenance and upgrades since the mid-1970s (Deverel, Bachand, et al. 2016a). Ongoing subsidence increases the risk of future levee failures and threatens the state's water supply, augmenting hydraulic forces against levees and exacerbating seepage, which can erode levee foundation materials and degrade levee stability over time (Deverel, Bachand, et al. 2016a). Alongside risks to the state's water supply, farming on deeply subsided Delta organic soils has become less viable and more economically challenging. Deverel et al. (2015), for example, reported that the extent of non-farmable and marginally farmable land in the Delta increased linearly about ten-fold from 1984 to 2012—from about 274 to 2,800 hectares (ha).

Scientists, resource managers, and policy-makers have increasingly focused on the potential for alternate land uses in the Delta to (1) stop or reverse subsidence, (2) sequester carbon and reduce GHG emissions, and (3) restore natural processes and ecosystems to promote recovery of imperiled species. Governing legislation established **improving water-supply reliability** and **restoring ecosystems** while **preserving the region's unique cultural values** (such as its agricultural heritage) as coequal goals for the Delta under the Delta Stewardship Council (DSC) Delta Plan (DSC 2013). Additionally, a core strategy of the DSC's 2022 Amended Delta Plan is to "**protect land for restoration and safeguard**

against land loss" (DSC 2022a). Proactive steps can help protect and restore intertidal habitat, evaluate the feasibility of subsidence-reversal projects, and incorporate actions that reduce GHG emissions and mitigate land loss by reducing, halting, and reversing subsidence.

Increasing the extent of wetlands on organic soils in the Delta can reduce GHG emissions and mitigate subsidence (Miller et al. 2008; Deverel et al. 2014; Deverel, Ingrum, et al. 2016; Hemes et al. 2019; Deverel et al. 2020). The state has recognized these benefits in policy and planning documents that call for wetland restoration and conversion to rice on subsiding Delta islands. Legislation passed in 2017 and 2022 requires California to meet one of the world's most ambitious goals for reducing GHG emissions, bringing emissions in California to less than 40% of 1990 levels by 2030 and achieving carbon neutrality by 2045 (AB 1279, Muratsuchi). The California Air Resources Board (CARB) stated that the majority of soil carbon loss in California is attributed to oxidation of organic soils in the Delta (CARB 2018), and the Natural and Working Lands Climate Change Implementation Plan—developed to identify land-based methods to sequester carbon—set a target of restoring 2,500 to 2,800 acres (1,000 to 1,100 ha) of Delta wetlands per year to stop carbon losses associated with soil oxidation (CNRA et al. 2019). More recently, in the 2022 Scoping Plan for Achieving Carbon Neutrality (CARB 2022), CARB included the creation of large areas of Delta wetlands and rice fields to reduce GHG emissions.

In addition to GHG and subsidence-mitigation benefits, wetland restoration and rice cultivation can restore lost ecosystem functions and reduce risks to the state's water supply. Flooded agriculture offers vital habitat for migratory waterbirds along the Pacific Flyway (Stralberg et al. 2011; Dybala et al. 2020), and the value of tidal and non-tidal wetlands for habitat and food-web support has been well documented in the literature (Howe et al. 2014; Colombano et al. 2021; Woo et al. 2021). On subsided islands, Deverel, Bachand, et al. (2016) demonstrated that thicker peat is associated with lower probability of levee failure; model results indicated that levee failures become more likely as marsh deposits thin to less than 3 or 4 m, and failure risk is exacerbated where levees are higher above the land surface. These results indicate that managed wetlands can reduce the future likelihood of levee failure by stopping subsidence and building peat elevations adjacent to levees.

Meeting the Delta's coequal goals will require future land-use changes that target these multiple management objectives while also providing income on working lands, as described in the Delta Plan (DSC 2013). Future land-use mosaics that include tidal wetlands, rice fields, and non-tidal peat-building wetlands managed for subsidence reversal offer a combination of habitat benefits, subsidence and GHG mitigation, and revenue from rice and the sale of carbon offsets (Whipple et al. 2022). To develop such well-balanced restoration plans, scenario-based planning can compare predicted outcomes of alternative land-use mosaics and identify where land-management decisions offer synergistic benefits or trade-offs between two or more objectives. Such information can be used at the landscape scale to define priorities for land-use decisions and define meaningful targets for ecological restoration, subsidence mitigation, and GHG emissions reductions. For Staten Island, for example, an analysis of alternative land-use scenarios identified where well-sited conversions to tidal marsh, non-tidal wetlands, and rice cultivation can reduce GHG emissions by over 30% and reverse elevation losses, while sustaining net revenues commensurate with existing land uses (primarily corn cultivation) (Deverel et al. 2017; Whipple et al. 2022).

To explore potential benefits of large-scale wetland creation and restoration, this study evaluated the effects of Delta land-use scenarios on peat carbon stocks, GHG emissions, and other ecosystem functions. We sought to answer the following questions:

1. What was the mass of peat carbon that was stored during the Holocene and lost since the 19th century?

https://doi.org/10.15447/sfews.2024v22iss2art3

2. What is the potential upper bound for net GHG benefits and peat carbon accumulation through wetland restoration and rice cultivation in the Delta?

3. What magnitude of GHG emissions reductions and peat carbon accretion could existing Delta wetland-restoration and rice-farming targets achieve?

4. How can the configuration of wetland restoration and rice cultivation be optimized for GHG mitigation and other restoration goals?

To address these questions, we developed a new analysis platform that integrates local peat core data and peat thickness mapping, historical and modern digital elevation models (DEMs), land-cover mapping, process-based vertical accretion and subsidence models, locally specific GHG emission factors, and additional spatial metrics of ecological function. This analysis tool allowed us to assess the effects of historical and future land-use changes on peat carbon stocks, subsidence, GHG emissions, and other Delta-specific functions for ecosystems, water supply, and people.

MATERIALS AND METHODS

Overview of Scenarios

To evaluate the effects of historical land-use change and potential future restoration on peat carbon stocks, GHG emissions, and other landscape functions in the Delta, we defined a set of seven large-scale land-cover and land-use scenarios. Scenarios spanned historical conditions, modern conditions, and five theoretical future configurations of wetland restoration and rice farming meant to assess the theoretical potential for future GHG mitigation, and compare existing targets for Delta wetland creation/restoration for GHG, subsidence, or habitat benefits (Table 1), elaborated as follows:

1. We defined the ***Historical*** scenario as the early 1800s Delta, before widespread diking and dredging of organic soils that began in the 19th century. Land cover in this scenario was dominated by tidal wetland (Whipple et al. 2012), underlain by thick peat deposits that developed over ~6,700 years (Drexler, de Fontaine, and Brown 2009).

2. We defined the ***Modern*** scenario to represent the contemporary Delta, comprised of the existing configuration of land uses, land-cover types, and infrastructure, as well as existing land surface elevations and bathymetry, based on a 2017 tidally referenced Digital Elevation Model (DEM) for the Delta (DSC 2022b; SFEI 2022), 2016 fine-scale vegetation mapping from the California Department of Fish and Wildlife (CDFW) Vegetation Classification and Mapping Program (VegCAMP) (CDFW 2019), and 2016 crop mapping from LandIQ (CDWR and LandIQ 2020).

Theoretical Future Configurations

3. We defined the ***Reference*** scenario to represent business-as-usual future conditions in which the existing configuration of land uses were maintained.

4. We defined the ***Maximum Potential*** scenario to represent the potential upper bound for wetland restoration to provide GHG and subsidence benefits and intertidal habitat. In the *Maximum Potential* scenario, any site not classified as urban or barren in the *Reference* scenario was converted to tidal or non-tidal wetland, with tidal wetland at intertidal elevations and non-tidal peat-building wetland in subsided areas.

5. ***GHG 1*** represented a highly ambitious scenario focused primarily on GHG mitigation. *GHG 1* added 17,000 ha of non-tidal peat-building wetland and 13,900 ha of rice fields, based on the extent of additional (above current commitments) freshwater wetland restoration in Scenario 1 from California's 2022 Scoping Plan for Achieving Carbon Neutrality.

6. ***GHG 2*** represented a more moderate scenario focused on GHG mitigation, based on additional wetland restoration in California's

Table 1 Description of future scenarios targets for tidal wetland, non-tidal peat-building wetland, and rice cultivation

Future scenario	Land-cover type	Scenario target
Reference	Tidal wetland	Maintain existing
	Non-tidal peat-building wetland	Maintain existing
	Rice field	Maintain existing
Maximum Potential	Tidal wetland	Expand to all available intertidal[a]
	Non-tidal peat-building wetland	Expand to all available subsided[a]
	Rice field	Maintain existing
GHG 1	Tidal wetland	Maintain existing
	Non-tidal peat-building wetland	Add 17,000 ha
	Rice field	Add 13,900 ha
GHG 2	Tidal wetland	Maintain existing
	Non-tidal peat-building wetland	8,480 ha
	Rice field	Add 6,940 ha
GHG-Habitat	Tidal wetland	Add 13,200 ha at intertidal elevations
	Non-tidal peat-building wetland	Add 6,680 ha (including 1,400 ha at shallowly subsided elevations)
	Rice field	Add 5,420 ha

a. Excludes land classified as urban or barren.

2022 Scoping Plan. *GHG 2* added 8,480 ha of non-tidal wetland for subsidence mitigation and 6,940 ha of rice fields.

7. The ***GHG-Habitat*** scenario was based on subsidence reversal and tidal wetland performance measures from the Delta Plan Draft Ecosystem Amendment (PM 5.2, 4.12, and 4.16; DSC 2013; DSC 2022a), which call for 32,500 acres (13,200 ha) of additional tidal habitat and 30,000 acres (12,100 ha) of subsidence mitigation—3,500 acres (1,400 ha) of which must be located at shallowly subsided elevations to provide tidal reconnection. We assumed that 55% of the subsidence mitigation was non-tidal peat-building wetland (6,680 ha), and we assumed the other 45% was rice fields (5,420 ha) (matching the ratio of peat-building wetland to rice field area used in *GHG 1* and *GHG 2*).

We defined the study extent for all scenario analyses as the historical extent of tidal wetland within the legal Delta mapped by Whipple et al. (2012). We developed GIS layers for all scenarios, based on existing (or historical) conditions and future-scenario acreages of additional non-tidal peat-building wetland, rice, and tidal wetland (Table 1). In all future scenarios, new wetland and rice was sited to optimize GHG emissions reductions, and areas not converted to wetland or rice were assumed to maintain *Reference*-scenario land uses. Appendix A[1] describes the optimization procedure.

Historical and Modern Peat Carbon Storage

To estimate changes in peat carbon stocks since the early 1800s, we derived maps of historical and modern peat thickness, and used a synthesis of peat carbon density data from soil cores taken from the Delta to create maps of peat carbon storage in the historical and contemporary Delta. The area of historical peat was defined for this study to equal the extent of historical tidal wetland, which was underlain primarily by peat and peaty mud with high organic matter content (Atwater and Belknap 1980). To delineate historical tidal wetlands and the historical channel structure, we used historical ecology mapping from Whipple et al. (2012).

1. *https://www.sfei.org/sites/default/files/biblio_files/Methods%20supplement%20Vaughn%20et%20al.%202024.pdf*

https://doi.org/10.15447/sfews.2024v22iss2art3

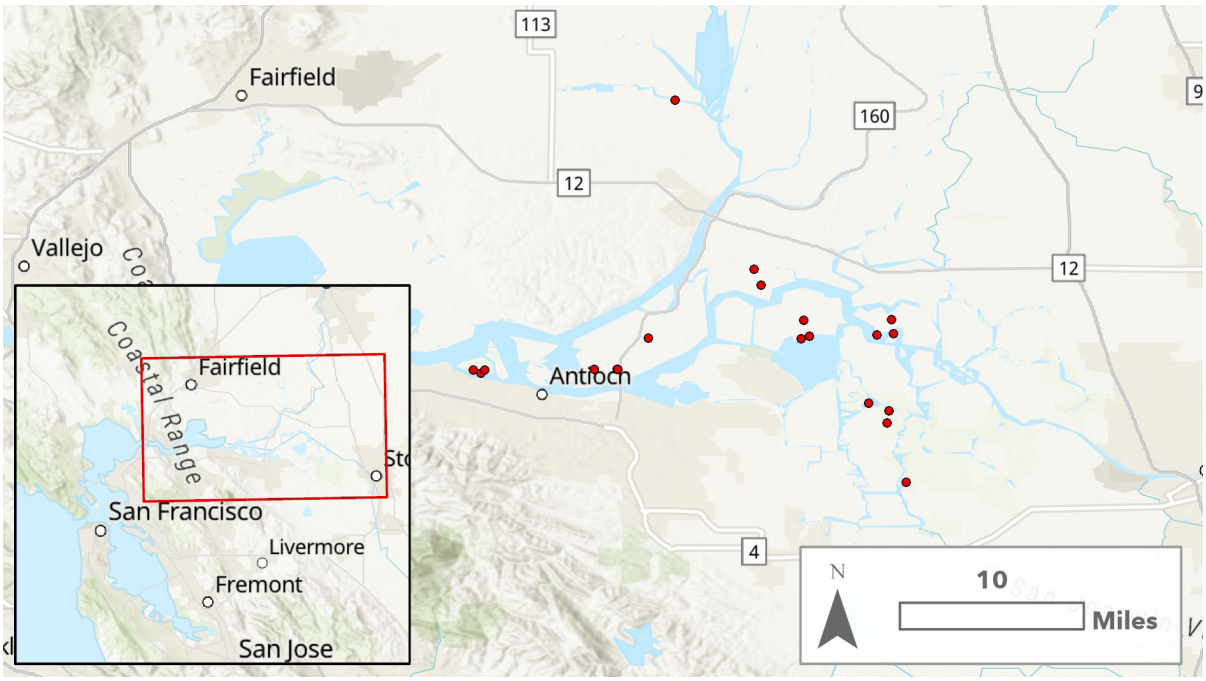

Figure 1 Sampling locations of peat cores used in peat core data synthesis

We developed a map of modern-day peat thickness from interpolated borehole data (Deverel and Leighton 2010) and 2017 land surface elevations (CDWR and USGS 2019). To map *Historical*-scenario peat thickness, we combined this modern peat thickness and elevation model with a historical DEM developed from maps of historical (ca. 1800) land cover and historical bathymetric data, including US Coast Survey (Survey of the Coast) hydrographic sheets and early river surveys (Robinson et al. 2014; Safran 2014). Where historical land surface elevations were greater than modern elevations, we assumed differences were the result of peat oxidation, compaction, and channel dredging (Drexler, de Fontaine, and Deverel 2009; Deverel et al. 2010; Robinson et al. 2014). Where historical tidal wetlands extended beyond the current extent of peat deposits, we assumed peat had likely been lost completely as a result of oxidation following wetland drainage. In these sites, we defined the historical elevation of the base of the peat to be equal to the current land surface elevation. This definition assumed that loss of peat volume was the primary source of elevation changes in this area since the early 1800s.

To map estimated *Historical*- and *Modern*-scenario peat carbon stocks, we applied carbon densities from a synthesis of peat core measurements to the historical and modern peat thickness maps. All peat core data used in this analysis were previously collected in historical tidal wetlands as part of five separate datasets in the Delta (Figure 1) that include ten cores from remnant tidal wetlands and thirteen from sites that have been drained and farmed. Deep cores ranging from 4 to 9 m in depth were collected from remnant marsh sites on Browns Island, Franks Wetland, Mandeville Tip, and Bacon Channel Island in 2005 and 2007 (Drexler, de Fontaine, and Brown 2009). Deep cores from 160 to 380 cm long were collected from levees and the centers of farmed islands, including Bacon Island, Venice Island, Sherman Island, and Webb Tract (Drexler, de Fontaine, and Deverel 2009). Cores 0.5 m in length from Browns Island were collected in 2010 by Callaway et al. (2012). Peat cores 0.5 m in length were collected from Lindsey Slough and

Middle River in 2018 (Drexler et al. 2021). Cores ranging from 0.6 to 0.8 m in length were collected from farmed sites on Twitchell and Sherman Island (Craig et al. 2017; Anthony and Silver 2020). Further information on coring procedures and measurements of % organic carbon (OC) and bulk density can be found in each of the above papers.

Soil cores from remnant sites exhibited some variation by depth in OC density. However, only four of the ten cores in this category included samples below the surface 0.5 m, so we lacked sufficient data to identify representative trends in OC density depth profiles. Instead, we calculated a single depth-aggregated average OC density across all remnant tidal wetland cores. Data from each core were binned into 10-cm slices, and the mean OC density was calculated for each bin. Empty bins were gap-filled using the average of OC density values in the nearest upper and lower bins with a reported OC density. Empty bins at the top or base of the profile were not gap-filled. With gap-filled profiles, we calculated the depth-averaged OC density of each profile, with soil core depths ranging from 0.5 to 9.2 m. Where multiple cores were collected from a particular island, we calculated the island-level mean as the average of individual core OC densities and averaged island-level means to determine the mean OC density for this category of peat (defined as ***intact*** **peat, representative of peat in intact, non-subsided profiles**).

Depth profiles from farmed island cores indicated particularly high OC densities in surficial soils. Shallow samples in these cores had high values for both bulk density and loss on ignition (LOI%) such that bulk density observations were higher than would be predicted from an established ideal mixing model between organic and mineral components in wetland sediments (Morris et al. 2016), using coefficients for self-packing densities derived from local core data (Morris et al. 2022)—an effect we did not observe at depth in the cores. To account for this effect, we defined ***altered*** peat in farmed sites as **surficial peat in which the measured bulk density exceeded the model-predicted bulk density by 30% or greater.** The base of this *altered* peat layer was found to range in depth among cores from 37.5 to 125 cm (mean = 78.8 ± 31.6 cm). Sensitivity tests indicated that results of the core data synthesis and Delta-wide peat carbon analysis were not sensitive to the choice of cut-off value between 20% and 35%. *Altered* peat within each farmed core was binned into 5-cm slices, and the overall mean OC density was calculated according to the same methods as *intact* peat.

Surface elevations of farmed island cores ranged between –4.4 m and –7.3 m relative to local mean sea level (MSL). In these deeply subsided sites, peat deposits below the *altered* peat layer included only the lower third to half of the original peat profile. We defined this category of peat as ***deep subsided*** peat, representative of **remaining peat on subsided islands below the altered surficial layer.** For each farmed-island core, we binned *deep subsided* peat into 10-cm slices and calculated OC density as with *intact* and *altered* peat.

With the eight farmed cores spanning *altered* and *deep subsided* categories, we tested whether differences in OC densities from *altered* and *deep subsided* were statistically significant. Using a linear mixed-effects model with peat class as a fixed effect and core as a random effect, we found that OC density values differed significantly between the two peat classes ($P << 0.001$). OC density values were log-transformed to meet model assumptions. Statistical modeling and significance testing were performed in R version 4.0.2 "Taking Off Again" (R Core Team 2020) using the packages lme4 (Bates et al. 2014) for modeling and lmerTest (Kuznetsova et al. 2014) for significance testing.

We applied peat carbon densities to the mapped peat to estimate peat carbon storage in the *Modern* and *Historical* scenarios. For the *Historical* scenario, we applied the *intact* peat carbon density to all peat deposits. For the *Modern* scenario, we categorized peat as intact peat, altered peat, or deep subsided peat, according to the degree of subsidence, land-cover type, and depth in the profile. In tidal wetland areas, we classified peat deposits as *intact* peat. In other sites, we classified the surface 79 cm as *altered* peat. Where surface elevations were deeply subsided to 2.4 m below mean lower low water

https://doi.org/10.15447/sfews.2024v22iss2art3

(MLLW), we classified peat layers below the *altered* category as *deep subsided* peat. Elsewhere, we classified peat below the surface 79 cm as *intact* peat, given the lesser degree of subsidence, as well as inclusion of shallow, relatively recent peat deposits in the remaining peat profile.

Future Scenario Modeling

For each of the five future land-use scenarios, we used a combination of models and emission factors to estimate changes in elevation, carbon stocks, and GHG emissions. We ran scenarios for 40 years from 2017 to 2057, assuming 34 cm (1.1 ft) of sea level rise (SLR) between 2000 and 2060, which is the high-likelihood SLR prediction from the 2018 Ocean Protection Council guidelines (OPC 2018). The rate of SLR was assumed to increase through time from 2000 to 2060 according to a quadratic model, $MSL_t = MSL_0 + at + bt^2$ where MSL_t and MSL_0 are MSL at times t and time 0, using a rate of SLR at time 0 of 0.28 cm yr^{-1} to solve for a and b. This annual increase was used to define annual sea level increases between 2017 and 2057.

Coastal Wetlands Equilibrium Model

We used the Coastal Wetlands Equilibrium Model (CWEM) to evaluate vertical accretion and carbon accumulation in areas classified as tidal wetland. An updated version of the Marsh Equilibrium model (MEM; Morris and Bowden 1986; Morris et al. 2012), CWEM is a 2-D cohort model that was recently adapted for the Delta (Morris et al. 2021; Morris et al. 2022), which predicts the change in wetland elevation in annual time-steps that results from the balance of vegetation biomass growth, sediment accumulation, decomposition, and compaction under SLR. To align scenario modeling with local tidal datums modeling, we used predicted tidal datums from the DSC's Delta Adapts Climate Change Vulnerability Assessment (DSC 2021a, 2021b) to define two characteristic SLR regions and three tidal-amplitude regions. For initial marsh surface elevation, we used a 2017 tidally referenced DEM for the Delta (DSC 2022b; SFEI 2022) to define six elevations bands centered at –90 cm, –60 cm, –30 cm, 0 cm, 30 cm, and 60 cm relative to mean tide level (MTL). A full list of CWEM parameters and values used in this analysis is provided in Appendix D[2].

We ran CWEM for all combinations of parameter values for the 40-year period beginning in 2017 (the most recent year for which a DEM was available). We used results from CWEM model runs to map predicted scenario vertical accretion according to SLR region, tidal-amplitude region, and initial marsh elevation. We converted vertical accretion to carbon accumulation using the carbon density value for *intact* peat derived from the peat core synthesis.

SUBCALC^2 Model

We used the SUBCALC^2 model to estimate future elevation and carbon losses in areas undergoing subsidence, defined in this analysis as sites underlain by organic or highly organic mineral soils that are classified as cropland, pasture, grassland, or seasonal wetland. SUBCALC^2 was originally developed by Deverel and Leighton (2010), updated in 2016 (Deverel, Ingrum, et al. 2016), and further updated and calibrated in 2021 and 2022 using eddy covariance and subsidence data in the Delta. SUBCALC^2 uses Michaelis–Menten kinetics to simulate microbial oxidation within organic and highly organic mineral soils under projected warming, with primary inputs including depth to groundwater, soil organic matter content above the water table, soil organic matter content below the water table, and thickness of the remaining peat. SUBCALC^2 was run for the 40-year model period from 2017–2057 using gridded model inputs across the Delta analysis area. Model outputs include change in elevation and net carbon flux (equal to carbon losses or CO_2 emissions from peat oxidation).

SEDCALC Model

We used the SEDCALC model to predict peat carbon accumulation in areas classified as non-tidal peat-building wetland. The SEDCALC model was originally developed by Callaway et al. (1996) and adapted by Deverel et al. (2014) to integrate Delta-specific data and simulate vertical accretion in managed non-tidal wetlands. SEDCALC

2. *https://www.sfei.org/sites/default/files/biblio_files/Methods%20supplement%20Vaughn%20et%20al.%202024.pdf*

predicts organic matter accumulation and vertical accretion, with primary model inputs including organic and mineral particle densities and time-varying surface organic matter and mineral sediment inputs, organic matter decomposition rates, belowground organic matter production and consolidation, and initial and limiting porosities. For non-tidal wetlands in subsided areas, we ran SEDCALC for the 40-year period from 2017 to 2057. In shallowly subsided areas, modeled accretion stopped if the surface elevation caught up with the increasing tidal datum.

Emission Factors

We used an emission factor approach to estimate net GHG exchanges and carbon stock changes in other land-cover types. We based estimates on literature-reported values for carbon sequestration/loss, net CO_2 emissions or uptake, methane (CH_4) emissions, and nitrous oxide (N_2O) emissions, using local data where available.

For wetlands not modeled with CWEM or SEDCALC, we assumed a carbon accumulation rate of 17 g C m^{-2} yr^{-1}—the rate reported by Bridgham et al. (2006) for freshwater mineral-soil wetlands. For agricultural sites underlain by mineral soils, we used a carbon accumulation value from Kroodsma and Field (2006) of 11 g C m^{-2} yr^{-1}. In grassland, savanna, and oak woodland sites underlain by mineral soils, we used a soil carbon loss rate of 38 ± 52 g C m^{-2} yr^{-1} based on grassland sites in Ma et al. (2007). For Bridgham et al. (2006) and Kroodsma and Field (2006), we assumed a low level of confidence, applying a 95% uncertainty range of 100% (i.e., 95% confidence that the actual value is within the estimate ± 100%). We assumed carbon uptake or losses from rice fields to be negligible (Hatala et al. 2012; Knox et al. 2015). For all land-cover categories, we assumed the net CO_2 uptake or emission rate to equal the annual change in carbon stock converted to units of CO_2. Because this calculation is based on simulated carbon stock changes, net CO_2 uptake estimates for tidal wetlands account for carbon lost to lateral fluxes (Arias–Ortiz, Oikawa, et al. 2021).

We based CH_4 emissions for scenario analyses on literature-reported values specific to each land-cover type. We assigned non-tidal peat-building wetlands a CH_4 emission rate of 63 ± 5.1 g CH_4 m^{-2} yr^{-1}, based on observations from impounded wetlands on Twitchell and Sherman islands (Hemes et al. 2019). Tidal wetland sites were assigned a CH_4 emission rate of 11 (+6.6 or –3.0) g CH_4 m^{-2} yr^{-1} for all scenarios—the mean emission rate from freshwater and oligohaline sites with mean annual temperature ≥19°C from Arias–Ortiz, Wolfe, et al. (2021). For peatland pastures, we used an annual CH_4 emission rate of 8.77 ± 4.39 g CH_4 m^{-2} yr^{-1} based on the per-head emission rate from the 2006 Intergovernmental Panel on Climate Change (IPCC) guidelines for GHG inventories (53 kg CH_4 $head^{-1}$ yr^{-1} ± 30% to 50%; Dong et al. 2006), and the reported cattle-stocking densities in the Delta (median = 1.6 cows ha^{-1}). We assigned rice fields a CH_4 emission rate of 16 ± 3 g CH_4 m^{-2} yr^{-1} based on rates reported from Twitchell Island (Hemes et al. 2019). Croplands (excluding rice) and subsiding non-agricultural grasslands were assumed to emit negligible CH_4 (Hemes et al. 2019). Finally, we assigned other non-tidal wetland types a value of 7.6 ± 3.9 g CH_4 $m^{-2}yr^{-1}$, the CH_4 emission rate for freshwater wetlands reported in Bridgham et al. (2006). Using the 100-year, global-warming potential of 28 (Myhre et al. 2013), we converted CH_4 emission rates to units of CO_2 equivalents (CO_2e).

We estimated emissions of N_2O for croplands, pasture, and subsiding peatlands, where N_2O is produced via organic matter oxidation and/or nitrification or denitrification of fertilizer or manure (Signor and Cerri 2013; Verhoeven et al. 2017). We used a distinct set of approaches for sites underlain by organic or highly-organic mineral soils (soil organic matter ≥ 6%) vs. mineral-soil sites. For pasture on organic soil, we applied a N_2O emission rate of 3.8 ± 2.0 g N_2O m^{-2} yr^{-1} based on measurements from Sherman Island (Teh et al. 2011). Rice cultivation on organic soil was modeled using a log-linear relationship between percent soil organic carbon and N_2O emissions observed in previously drained histosols on Twitchell Island

https://doi.org/10.15447/sfews.2024v22iss2art3

(Ye et al. 2016). For other subsiding (organic-soil) areas, we estimated N_2O emissions from SUBCALC[2]-predicted CO_2 emissions, using a constant relationship between organic matter oxidation and N_2O emissions, where N_2O (kg CO_2e) = 0.153 × CO_2 (kg CO_2) (Deverel et al. 2017). For pasture and rice in mineral-soil areas, we used N_2O emission rates reported in Verhoeven et al. (2017) (1.79 ± 0.49 and 0.14 ± 0.093 g N_2O m^{-2} yr^{-1} respectively), and for other mineral-soil cropland sites we used a value of 0.33 ± 0.04 g N_2O m^{-2} yr^{-1} (De Gryze et al. 2010; Verhoeven et al. 2017). N_2O emissions were converted to CO_2e using the 100-year global warming potential of 265 (Myhre et al. 2013).

Scenario Analysis with the Landscape Scenario Planning Tool (LSPT)

The models and emission factors described above were integrated into a GIS-based scenario analysis platform, the Landscape Scenario Planning Tool (LSPT). For a specified land-use scenario, the LSPT assigns model(s) and/or emission factor(s) according to the scenario land-cover type, degree of subsidence, and soil classification (organic vs. mineral soil). The LSPT then produces spatially explicit estimates of subsidence or vertical accretion; carbon accumulation or loss; GHG emissions or uptake (the sum of CO_2, CH_4, and N_2O in units of CO_2e); and GHG emissions reductions (the difference in emissions between the baseline and an alternative scenario) over the 40-year simulation period beginning in 2017.

We ran GIS layers for each of the five future scenarios through the LSPT, using the *Reference* scenario as the baseline against which GHG emissions reductions were calculated. In addition to GHG and subsidence-related metrics, the LSPT performs a suite of other spatially explicit analyses related to ecosystem function and existing land uses, which allow users to consider subsidence and GHG mitigation in a multiple-benefits framework. To evaluate each scenario's performance for other key functions related to the Delta coequal goals, we used the LSPT to evaluate metrics of wetland habitat configuration (marsh size and distance), habitat connectivity (wetland–water connections) and Delta as place (agricultural land uses). In all future scenarios, agricultural sites not converted to wetland were assumed to maintain the current distribution of pastureland, cropland, crop types, and agricultural practices, with the simplifying assumption that there were no indirect changes to the channel- and land-cover-type configuration from levee failures, infrastructure changes, or other such climate- or policy-driven events.

RESULTS

Historical, Modern, and Future-Scenario Elevation and Peat Carbon Stocks

We estimate that historical tidal wetlands in the Delta were underlain by 7.8 km^3 of peat before anthropogenic modifications in the 19th and 20th centuries (Figure 2). Between the *Historical* and *Modern* scenarios, we found that the Delta lost an estimated two-thirds of its historical peat (5.0 km^3) and half its historical peat carbon (140 million metric tons [megatonnes; Mt] C) from oxidation and compaction. Historical peat deposits covered an estimated 150,000 ha and stored 288 Mt C (95% CI = 259 to 317) (Table 2). In contrast, the Delta's modern peat deposits span ~95,000 ha, with a total estimated volume of 2.8 km^3 and carbon stock of 145 Mt C (95% CI = 117 to 172). We found that 20% of historical peat losses (1.0 km^3) occurred in areas where peat is no longer present, which are primarily at the northern, eastern, and southern margins of the Delta. In comparison, the remaining 4.0 km^3 of peat was lost from thicker, extant peat deposits in the central and western Delta.

Delta-wide maps of peat carbon storage indicate variability in the depth of peat deposits and broad differences in peat carbon density with land use and depth. From the peat core analysis, we found that peat collected from farmed sites had greater carbon density than that from remnant tidal wetlands, particularly in surface layers (Table 3). Across cores from remnant tidal wetland sites, OC density of *intact* peat varied spatially from 30 ± 4.6 kg C m^{-3} from a Middle River Marsh core to 46 ± 6.5 kg C m^{-3} from a core collected on Browns Island, with an overall mean OC density of 36 kg C m^{-3} (95% CI = 32 to 40) (Table 3). From

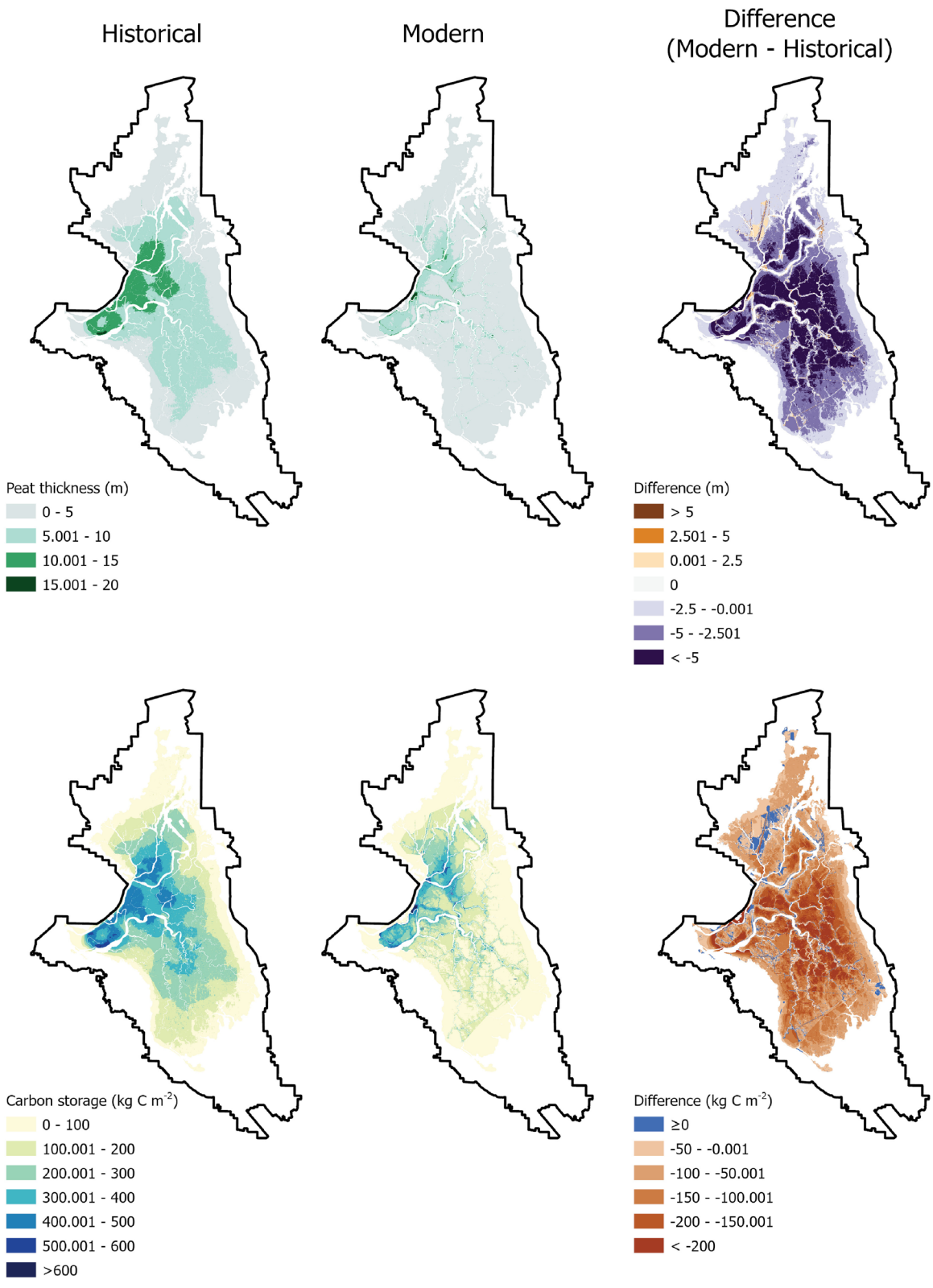

Figure 2 Mapped changes over time in peat thickness and peat carbon storage in the Sacramento–San Joaquin Delta. *Historical* maps illustrate modeled peat conditions in the early 1800s, and *Modern* maps depict estimated peat depths and carbon stocks in 2017. Mapped differences show changes in peat volume and carbon from oxidation and compaction, where negative values indicate a net loss over time of peat or peat carbon.

https://doi.org/10.15447/sfews.2024v22iss2art3

Table 2 Peat carbon density estimates for the Sacramento–San Joaquin Delta based on analysis of peat cores collected in remnant tidal marshes and subsided farmed islands[a]

Peat category	Land cover type	Mean peat carbon density (kg C m^{-3})
Intact	Remnant tidal marsh	37 ± 5.9 (n = 10)
Altered	Subsided farmed islands	97 ± 37 (n = 5)
Deep subsided	Subsided islands	46 ± 4.2 (n = 4)

a. Error ranges represent standard deviations across island-level means included in the overall average for each peat category. *N* represents the number of islands over which data were summarized for each peat category.

Table 3 Peat carbon stocks in the *Historical* Delta (early 1800s), the *Modern* Delta (2010s), and future wetland-restoration and rice-farming scenarios

Scenario	Peat carbon storage Mt C (95% CI)
Historical (early 1800s)	279.9 (248.8–313.6)
Modern (2010s)	143.6 (116.3–170.9)
Reference (2057)	135.3 (105.9–165.6)
Maximum Potential (2057)	167.2 (139.9–194.5)
GHG 1 (2057)	144.4 (116.0–173.0)
GHG 2 (2057)	140.9 (112.1–170.0)
GHG-Habitat (2057)	140.2 (111.4–169.5)

the eight cores included in the *deep subsided* peat category, we calculated a mean OC density of 46 kg C m^{-3} (95% CI = 42 to 50), with a range across cores of 38 ± 8.4 to 56 ± 6.4 kg C m^{-3}. In comparison, the *altered* peat category—defined as surficial peat from farmed cores in which observed bulk density was at least 30% greater than predicted from a locally-derived version of the LOI-bulk density relationship (Morris et al. 2016)—exhibited a broader range of OC densities, which ranged across cores by an order of magnitude: from 25 ± 15 kg C m^{-3} from a Twitchell Island alfalfa field to 200 ± 19 kg C m^{-3} from a core collected near the center of Bacon Island. We calculated a mean OC density of *altered* peat of 97 kg C m^{-3} (95% CI = 64 to 130), roughly twice as high as *deep subsided* peat and ~3x as high as the *intact* peat category. (See Appendix B[3] for further detail.).

Results of future-scenario modeling showed that with no changes to the current land-cover configuration (the *Reference* scenario), an additional 0.17 km^3 of peat may be lost during the next 40 years as a result of ongoing oxidation, with modeled future carbon losses of 8.3 Mt C (Table 3; Figure 3) which is equal to the carbon stored in over 40,000 ha of forest (USEPA 2021). In the *Modern* Delta, 65,319 ha of land are deeply subsided, defined here as having surface elevations more than 3 m below MTL (Table 4). With continued subsidence, we found that the extent of deeply subsided land increased

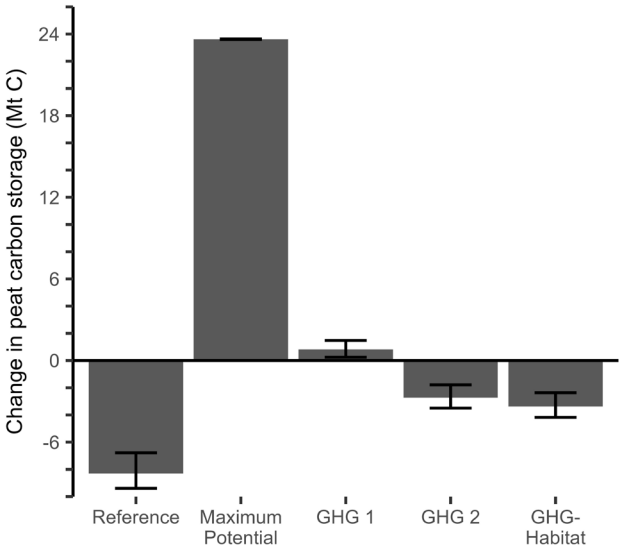

Figure 3 Future scenario cumulative change in peat carbon storage over the 40-year modeling period (2017–2057). *Error bars* represent standard errors propagated from error ranges from the SUBCALC[2] model, the Coastal Wetlands Equilibrium Model (CWEM), and peat core data.

by ~10,000 ha in the *Reference* scenario over the 40-year simulation period (2017–2057) as a result of further elevation losses in more shallowly subsided sites as well as a reduction in the extent of land at intertidal and terrestrial elevations.

Results of the *Maximum Potential* scenario provide upper-bound estimates for carbon sequestration, subsidence mitigation, and GHG emissions reductions through extensive restoration of tidal and managed wetlands. Scenario results

3. *https://www.sfei.org/sites/default/files/biblio_files/Methods%20supplement%20Vaughn%20et%20al.%202024.pdf*

Table 4 Extent of land subsidence at the end of the 40-year modeling period (2057)[a]

Scenario	Deeply subsided land area (>3 m below mean tide level) (ha)	Shallowly subsided land area (3 m below mean tide level to mean lower low water) (ha)	Intertidal land area (mean lower low water to mean higher high water) (ha)	Tidal-terrestrial land area (above mean higher high water) (ha)
Modern	65,319	52,879	17,884	10,223
Reference	72,892	51,547	15,659	6,438
Maximum Potential	52,246	54,376	32,507	7,270
GHG 1	69,474	54,765	15,808	6,440
GHG 2	71,647	52,727	15,675	6,438
GHG-Habitat	72,110	51,690	16,246	6,441

a. Intertidal zone approximated using a mean tidal range of 1.1 m. *Maximum Potential* extent excludes 88 ha for which model-based subsidence or accretion values were unavailable.

indicate that a net soil carbon gain of 24 Mt over *Modern* scenario conditions could theoretically be achieved over a period of 40 years. This large-scale restoration of wetlands could rebuild 17% of the peat C that was historically lost and decrease the extent of deeply subsided land by over 20,000 ha (nearly 30%) relative to the *Reference* scenario (Tables 3 and 4). Of the remaining three wetland-restoration and rice-cultivation scenarios, the most ambitious in terms of overall acreage—*GHG 1*—resulted in a net gain in peat carbon over the *Modern* scenario of 0.8 Mt C over 40 years, reducing the extent of deeply subsided land by 3,400 ha relative to the *Reference* scenario. The other two scenarios—the *GHG 2* and the *GHG-Habitat* scenario—resulted in a net loss of carbon over the modeling period, and only modest reductions in the extent of deeply subsided land relative to the *Reference* scenario. In these two scenarios, peat carbon accretion in managed and tidal wetlands only partially offset carbon losses in subsiding agricultural areas, with net 40-year cumulative carbon losses of 3.4 Mt (*GHG-Habitat*) and 2.7 Mt (*GHG 2*).

Modern and Future GHG Emissions

Using the new "*Carbon and GHG Emissions*" module we developed for the LSPT, we found that if existing land uses are maintained (the *Reference* scenario), the Delta may have net annual GHG emissions of 1.2 Mt CO_2e yr^{-1} on average over the coming 40 years (Figure 4). In comparison, results of the *Maximum Potential* scenario indicate that at the upper bound the Delta could provide net GHG uptake from the atmosphere of 19,100 t CO_2e yr^{-1} over the 40-year modeling period. Given high baseline GHG emissions in the *Reference* scenario, maximizing wetland extents could thus provide a theoretical net GHG benefit of 1.2 Mt CO_2e yr^{-1} (95% CI = 1.0 to 1.4) relative to business-as-usual conditions (Figure 4).

The *GHG 1, GHG 2,* and the *GHG-Habitat* scenarios all provided substantial GHG emissions reductions compared with the *Reference* scenario, with the largest GHG emissions reductions in the *GHG 1* scenario (Figure 4B). In all three scenarios, however, the Delta remained a net source of GHGs to the atmosphere because of ongoing CO_2 emissions in subsiding areas and CH_4 emissions from wetlands (Table 5; Figure 4A). Results of these three intermediate scenarios were as follows:

- ***GHG 1*** provided the greatest GHG emissions reductions relative to the *Reference* scenario, with Delta-wide GHG emissions of 0.53 Mt CO_2e yr^{-1} (95% CI = 0.27 to 0.79) and annual GHG emissions reductions of 0.67 Mt CO_2e yr^{-1} (95% CI = 0.55 to 0.78) (Figure 4). In this scenario, the additional non-tidal peat-building wetlands and rice fields were distributed across portions of the Central and West Delta, where conversion to wetted land uses would eliminate the high baseline GHG emissions in the *Reference* scenario.

- ***GHG 2*** offered lower GHG benefits than *GHG 1*, given that it included only roughly half the acreage of managed wetland and rice from a

https://doi.org/10.15447/sfews.2024v22iss2art3

A Net annual GHG emissions for each future scenario

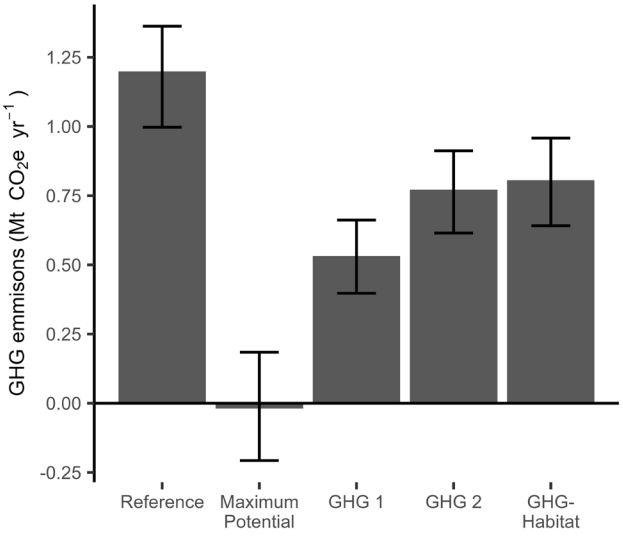

B Future scenario greenhouse gas emissions relative to the *Reference* scenario

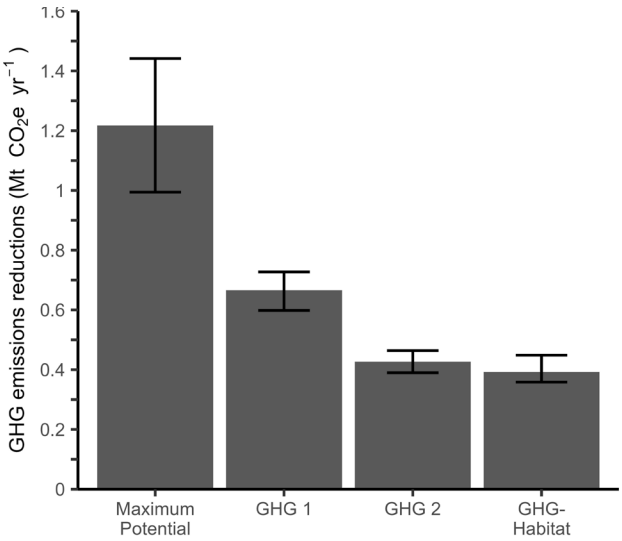

Figure 4 Future scenario greenhouse gas (GHG) emissions. Net GHG emissions (**A**) are expressed as the mean annual rate over 40 years in CO_2 equivalents, with positive values indicating a net emission from the ecosystem to the atmosphere. Annual GHG emissions reductions (**B**) were quantified as the difference in net GHG emissions between a given scenario and the *Reference* scenario.

subset of *GHG 1* locations (Table 5). Average Delta-wide GHG emissions modeled for this scenario were 0.77 Mt CO_2e yr^{-1} (95% CI = 0.46 to 1.05), demonstrating GHG emissions reductions of 0.43 Mt CO_2e yr^{-1} (95% CI = 0.35 to 0.50) relative to the *Reference* scenario (Figure 4).

- For the ***GHG-Habitat*** scenario, we estimated overall GHG emissions of 0.81 Mt CO_2e yr^{-1} (95% CI = 0.48 to 1.1), or GHG emissions reductions of 0.39 Mt CO_2e yr^{-1} (95% CI = 0.33 to 0.46) relative to the *Reference* scenario (Figure 4), which was not appreciably different from *GHG 2*. Unlike the other two *GHG* scenarios—which included only rice and non-tidal peat-building wetland—this scenario included tidal wetland restoration (Table 5), which was sited primarily near the margins of the Delta's historical tidal wetland footprint. The *GHG-Habitat* scenario additionally required that 1,400 ha (3,500 acres) of the additional non-tidal peat-building wetland be located at shallowly subsided elevations (defined as subsidence reversal for tidal reconnection). In contrast with the other two *GHG* scenarios, this placed a portion of the additional non-tidal wetland in sub-optimal sites for GHG emissions reductions, primarily near tidal wetland sites at the periphery of the study extent.

Other Metrics Quantified by the LSPT

In addition to GHG benefits and carbon sequestration, we evaluated metrics of marsh habitat, fish support, and agricultural land use associated with each scenario (Table 6). Relative to the *Reference* scenario, all four other future scenarios increased the total area of large marsh patches (contiguous regions of tidal and non-tidal emergent wetland), which provide greater habitat structural complexity and support larger population densities or greater occupancy of certain marsh wildlife species than small, discontinuous marsh areas (Spautz et al. 2005; Takekawa et al. 2006; Aylward et al. 2023). With the current configuration of land-use and land-cover types, marsh patches larger than 100 ha cover 4,806 ha across the Delta, and marsh

Table 5 Mean annual greenhouse gas (GHG) emissions of tidal wetlands, peat-building wetlands, and rice fields in future scenarios[a]

Future scenario	Land-cover type	Total area (ha)	Additional area (ha)	Mean annual net GHG emissions t CO_2e yr^{-1} (95% CI)
Maximum Potential	Tidal wetland	22,885	19,432	– 61,947 (– 89,146 to – 3,555)
	Non-tidal peat-building wetland	136,169	131,134	31,500 (– 300,399 to 363,432)
	Rice field	1,114	0	69 (42 to 97)
GHG 2	Tidal wetland	3,453	0	– 6,097 (– 11,928 to 6,493)
	Non-tidal peat-building wetland	13,296	8,497	4,291 (– 25,027 to 33,622)
	Rice field	9,543	7,072	37,953 (23,764 to 52,165)
GHG 1	Tidal wetland	3,453	0	– 6,097 (– 11,928 to 6,493)
	Non-tidal peat-building wetland	21,637	17,036	6,427 (– 45,824 to 58,693)
	Rice field	16,379	13,946	68,618 (42,948 to 94,329)
GHG-Habitat	Tidal wetland	15,518	12,756	– 40,224 (– 58,946 to 196)
	Non-tidal peat-building wetland in subsided areas	10,153	5,268	3,480 (– 17,100 to 24,074)
	Non-tidal peat-building wetland for tidal reconnection	1,428	1,428	537 (– 2,599 to 3,676)
	Rice field	8,066	5,469	31,326 (19,619 to 43,052)

a. For each scenario and land-cover type, mean annual GHG emissions include net emissions of CO_2, CH_4, and N_2O. Positive values indicate a net GHG emission from the ecosystem to the atmosphere (GHG source), and negative values represent a net GHG uptake (GHG sink).

patches larger than 500 ha span a total of 856 ha. In comparison, the *Maximum Potential* scenario would support a total of 158,181 ha of marsh in patches greater than 100 ha and 157,743 ha of marsh patches greater than 500 ha—an increase of nearly 200% over the *Modern* scenario. *GHG 1* includes 16,674 ha (>100 ha) or 5,177 ha (>500) of large marsh patches; *GHG 2* would support 10,276 ha (>100 ha) or 2,848 ha (>500 ha) of large marsh patches; and the *GHG-Habitat* scenario includes 17,836 ha (>100 ha) or 6,948 ha (>500 ha) of large marsh patches. Relative to the *Modern* and *Reference* scenarios, all four future land-use-change scenarios decreased the nearest neighbor distance between marshes, defined as the average distance from a given marsh site to another. With the current landscape configuration, marsh patches are on average 14 km from the nearest patch greater than 100 ha. This distance—a simple measure of habitat connectivity—decreased to 6.0 km for *GHG 2*, 3.9 km for *GHG 1*, 3.0 km for the *GHG-Habitat* scenario, and only 1.4 km for the *Maximum Potential* scenario.

The increase in tidal marsh in the *Maximum Potential* and *GHG-Habitat* scenarios also improved metrics of connectivity between channels and wetlands related to support for fish such as Delta Smelt and juvenile salmonids (Hammock et al. 2019; SFEI 2020). In the *Modern* and *Reference* scenarios, 8,925 ha of tidal marsh is within 2 km of open water in the channel network. In contrast, tidal marsh area within 2 km of open water spans 54,923 ha in the *Maximum Potential* scenario and 9,342 ha in the *GHG-habitat* scenario, likely improving the likelihood of foraging success by Delta Smelt and other fish that forage in tidal channels (Howe et al. 2014; Hammock et al. 2019). Similarly, the inclusion of tidal wetland restoration in future scenarios decreases the average distance along the channel that fish have to travel to reach the nearest large and connected wetland area (> 500 ha patch that is contiguous with the channel network) from 7 km in the *Modern* and *Reference* scenarios to 0.043 km in the *Maximum Potential* scenario. This configuration of marsh patches would likely increase the frequency with which juvenile salmonids find conditions suitable for their growth and survival (SFEI 2020). Although the *GHG-Habitat* scenario adds nearly 13,000 ha of tidal wetland, the distributed placement of this wetland at the margins produces only negligible reductions in the distance fish must travel along the channel to the nearest large wetland.

https://doi.org/10.15447/sfews.2024v22iss2art3

Converting existing land uses to tidal and non-tidal wetlands provides several ecosystem benefits in the Delta but also includes a trade-off with existing land uses. In the *Maximum Potential* scenario, conversion of all agricultural land in the study area to tidal or non-tidal wetland amounts to a loss of 114,814 ha of agricultural production, nearly 100,000 ha of which (85%) is classified as prime farmland by the California Department of Conservation's Farmland Mapping and Monitoring Program's 2018 database (CDC 2018). The inclusion of rice fields in the alternative future scenarios reduces the loss of agricultural land. For each of the two GHG scenarios, 51% of the land-use changes entail a loss of agriculture, with reductions in the extent of land under agricultural production of 15,719 ha and 8,001 ha for *GHG 1* and *GHG 2* respectively. For *GHG 1,* 85% of this lost agricultural land is classified as prime farmland; for *GHG 2,* 92%. The *GHG-Habitat* scenario entails a loss of 18,244 ha of land managed for agriculture—14,862 of which is prime farmland.

DISCUSSION

This study used a synthesis of models and data to evaluate changes in peat carbon stocks, GHG emissions, and other ecosystem functions between the past, the present, and future scenarios in the Sacramento–San Joaquin Delta. We used a novel approach to reconstruct historical peat carbon storage, and combined models of wetland vertical accretion, peat subsidence, and GHG emission factors to: (1) quantify the theoretical opportunity for carbon sequestration and GHG emissions reductions through wetland restoration, (2) evaluate the magnitude of potential benefits from alternative wetland-restoration and rice-farming scenarios based on existing targets, and (3) explore co-benefits and trade-offs between GHG benefits and other goals of land-use planners in the Delta.

Historical and Present-Day Carbon Stocks

Historical-scenario peat carbon stocks quantified in this study were 290 Mt C (95% CI = 260 to 320) (Table 3), a value that is 78 to 140 Mt C greater than previous estimates based on subsidence rates and accommodation space (Mount and Twiss 2005; Deverel and Leighton 2010; Drexler et al. 2019). These differences in estimated carbon stocks were driven primarily by differences in the estimated volume of historical Delta peat, given that the carbon density value of 37 kg C m^{-3} (95% CI = 33 to 41) that we used in this study (Table 3) was comparable to that used in previous estimates (34.2 to 41.0 kg C m^{-3}; Drexler et al. 2019). Our method of historical reconstruction measured a total volume of historical peat of 7.8 km^3, compared with previous estimates of 4.5 to 5.1 km^3 (Mount and Twiss 2005; Deverel and Leighton 2010).

The accommodation space methods used previously were limited to existing peat deposits, which are smaller at present than the full extent of historical tidal marsh (Whipple et al. 2012). In the North and South Delta in particular—in areas mapped as historical tidal marsh that are not currently underlain by organic soils (Deverel and Leighton 2010)—our analysis of historical and modern DEMs revealed substantial elevation losses since the early 1800s. Given the observed relationship between soil organic matter content and organic soil subsidence rates (Deverel and Rojstaczer 1996; Deverel and Leighton 2010), we attributed these elevation changes to the complete loss of historical peat as a result of organic matter oxidation (Figure 2). By extending the map of historical peat thickness beyond current peat deposits, we produced a map of peat for the *Historical* scenario that amounts to 37% to 92% more carbon than has been reported in previous first-order estimates (Drexler et al. 2019).

This study's estimate of *Modern*-scenario peat carbon storage was also higher than previously reported values. Compared with earlier estimates that peat deposits currently store between 69 and 110 Mt C (Drexler et al. 2019), we found that existing peat in the modern Delta stores an estimated 140 Mt C (95% CI = 120 to 170) (Table 3). In contrast with historical carbon estimates, we attribute this difference primarily to differences in the peat carbon densities used in the analyses rather than differences in peat volume. Our analysis of peat cores from farmed islands found

significantly higher carbon densities in surficial peat than in deeper layers or remnant wetland sites (Table 3), likely the result of compaction and other effects of farming on soil composition and structure. By applying the higher mean carbon density for the *altered* peat class to the top 79-cm-deep layer of peat (97 kg C m^{-3}, 95% CI = 64 to 130), we accounted for this effect in our analysis of modern peat carbon. This finding indicates that although roughly two-thirds of the peat column has been lost to subsidence (Drexler, de Fontaine, and Deverel 2009), high carbon densities in approximately the upper 1 meter of remaining peat mitigate (to a small degree) associated carbon losses.

Although our estimates of modern-day Delta peat carbon stocks were higher than previously reported, we found that roughly 50% more carbon has been lost from Delta peat than was previously estimated (145 compared with 83 to 100 Mt C; Drexler et al. 2019), given our higher estimates of peat carbon stocks in the *Historical* Delta. We were not able to capture several sources of uncertainty in this analysis, including uncertainty in historical elevations and interpolated peat basal elevations, historical extents of peat deposits, and the representativeness of available peat core data. However, as approximate values and an update to previous estimates, our findings suggest that peat oxidation in the Delta has led to a greater loss of carbon than was previously thought, contributing to the state's historical burden of GHG emissions from natural and working lands.

Multiple Benefits of Future Land-Use Scenarios

The *Maximum Potential* scenario represents the theoretical ecological potential to rebuild carbon stocks and mitigate subsidence through wetland restoration. While this scenario is the least likely of the five future scenarios because of its complete elimination of farming in the Delta, it serves to define the upper bound for theoretical carbon sequestration and GHG mitigation. We found that over a period of 40 years (2017 to 2057), an estimated 24 Mt C could be sequestered in Delta peat in the *Maximum Potential* scenario, or roughly 17% of the total peat carbon that has been lost to oxidation (Figure 3). In addition to sequestering carbon, expanding the wetted area in the Delta through wetland restoration and rice farming would provide a net GHG benefit relative to business-as-usual (*Reference*-scenario) conditions by reducing ongoing emissions (Figure 4). If all non-developed areas at or below intertidal elevations were converted to wetlands, we estimated that net biogeochemical GHG emissions from the Delta could be reduced by an estimated 1.2 Mt CO_2e yr^{-1} relative to the *Reference* scenario, converting the Delta from a 1.2 Mt CO_2e yr^{-1} GHG source to a 0.019 Mt CO_2e yr^{-1} GHG sink (Figure 4), and offsetting the emissions from ~260,000 gas-powered passenger cars (using the USEPA value of 4.6 metric tons [tonnes; t] CO_2e yr^{-1}; USEPA 2022). This figure highlights the scale of the opportunity for GHG mitigation in the Delta; even with substantial CH_4 production in freshwater impounded wetlands, tidal wetlands, and rice fields, halting ongoing peat oxidation in drained and subsiding sites provides an opportunity to mitigate climate change.

The potential for wetland restoration to reduce GHG emissions varies in magnitude across the Delta, primarily because of the spatial variability in baseline GHG emission rates. *Modern* and *Reference* scenario GHG emissions range substantially within and among islands according to differences in soil organic matter content, depth of the organic soil, depth of the water-table, and other key parameters that influence organic matter oxidation (Deverel and Leighton 2010). Across much of Bouldin Island, for example, estimated GHG emissions are greater than 6 kg CO_2e m^{-2} yr^{-1}, whereas most sites in the Delta emit between 0 and 4 kg CO_2e m^{-2} yr^{-1} (see Appendix G[4]). For this reason, strategic siting of restoration can offer particularly high benefits to mitigate for climate change and subsidence. Additionally, the GHG benefits of Delta restoration may not increase linearly with the acreage of land over which wetted conditions are restored. If parcels are ranked according to GHG mitigation potential, the incremental GHG mitigation benefit of additional restoration decreases with each restored parcel (Figure 5).

4. *https://www.sfei.org/sites/default/files/biblio_files/Methods%20supplement%20Vaughn%20et%20al.%202024.pdf*

https://doi.org/10.15447/sfews.2024v22iss2art3

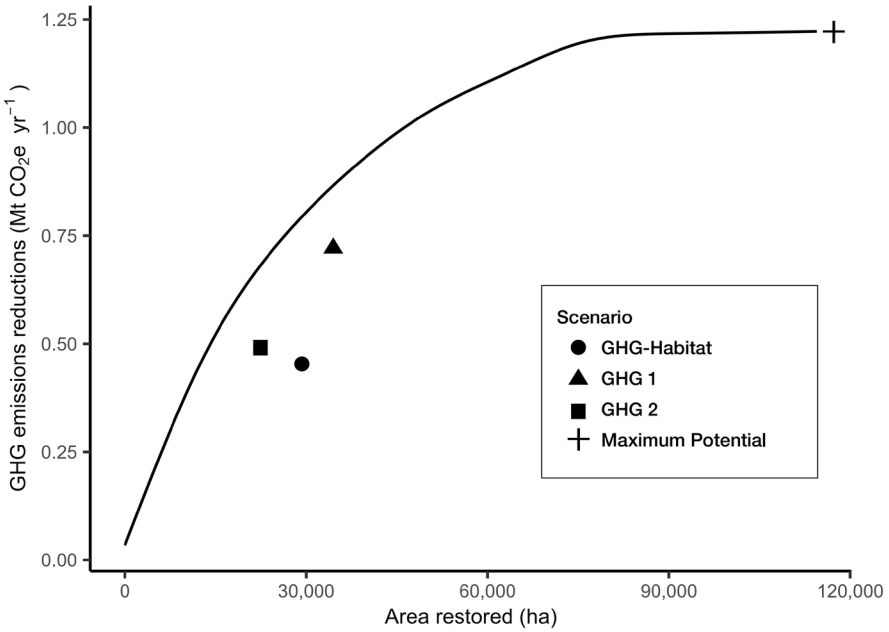

Figure 5 Change in potential greenhouse gas (GHG) benefits with cumulative restoration acreage. The *black line* shows how cumulative GHG emissions reductions change as additional parcels are converted to wetland in order from highest to lowest per-area GHG emission reduction according to results of the *Maximum potential* scenario. *Points* show the total GHG emissions reductions and acreages of additional wetland for the *Maximum potential*, *GHG 1*, *GHG 2*, and *GHG-habitat* scenarios. Scenarios deviate from the GHG optimum (*black line*) due to the inclusion of rice fields and/or tidal wetland in scenario wetland acreages.

Despite these diminishing returns, annual GHG emissions reductions continue to increase with additional restoration until ~75,000 ha have been converted to wetland—over twice the restoration area in *GHG 1* or the *GHG-Habitat* scenario, and nearly four times the restoration area of *GHG 2*. This indicates that existing restoration targets for the Delta capture only a fraction of the available opportunity for wetland restoration to support California's climate action goals. Even with the high restoration acreages included in *GHG 1*, considerably more potential remains for wetland restoration to reduce GHG emissions in the Delta.

Differences in the estimated per-area GHG benefit among scenarios depended on both the position of each scenario along the curve in Figure 5 and the portfolio of additional wetland—i.e., the acreages of tidal wetland, rice, and managed non-tidal wetland. Although the *GHG-Habitat* scenario, *GHG 1*, and *GHG 2* fall short of the maximum potential per-acre GHG benefit, they all represent ambitious restoration targets that would substantially reduce GHG emissions. We found per-area GHG emissions reductions of 16 t CO_2e ha^{-1} yr^{-1} for the *GHG-Habitat* scenario, 21 t CO_2e ha^{-1} yr^{-1} for *GHG 1*, and 28 t CO_2e ha^{-1} yr^{-1} for *GHG 2*. Even given the variability in benefits among scenarios, these per-area GHG emissions reductions are high relative to other land-management practices, demonstrating the great potential of wetland restoration in the Delta to support California's climate change mitigation goals. Based on analyses in California's Scoping Plan for Achieving Carbon Neutrality, achieving a comparable GHG benefit from other natural and working land-management practices would require >4 times as much cropland (regenerative agriculture and conservation) or >120 times the area of forests, shrublands, and grasslands (fuel reduction and restoration) (CARB 2022).

We found that all future restoration scenarios would increase the extent and quality of wildlife habitat by increasing the area of large marsh patches and improving metrics of landscape connectivity important for the movement of wildlife and resources (Table 6). Among *GHG 1*, *GHG 2*, and the *GHG-Habitat* scenario, the *GHG-Habitat* scenario provided the greatest increase in large marsh patches and metrics of landscape connectivity, primarily as the result of the inclusion of ~13,000 ha of tidal wetland (Tables 1 and 6). These marsh and connectivity metrics reflect the extent and quality of wildlife habitat. Marsh patches greater than 100 ha are more likely to support high densities of marsh birds (Spautz et al. 2005), and patches greater than 500 ha are

Table 6 Additional area and distance metrics of habitat quality, connectivity, and land use associated with future scenarios[a]

	Reference	Maximum Potential	GHG 2	GHG 1	GHG-Habitat
Area of marsh patches greater than 100 ha[1]	4,806 ha	158,181 ha	10,276 ha	16,674 ha	17,836 ha
Area of marsh patches greater than 500 ha[1]	856 ha	157,743 ha	2,848 ha	5,177 ha	6,948 ha
Average distance to nearest marsh patch greater than 100 ha[1]	14 km	1.4 km	6.0 km	3.9 km	3.0 km
Area of tidal marsh within 2 km of open water	4,636 ha	9,398 ha	4,636 ha	4,636 ha	5,053 ha
Average distance to nearest large connected wetland[2]	7 km	0.043 km	7 km	7 km	7 km
Loss of agriculture	—	114,814 ha	8,001 ha	15,719 ha	18,244 ha
Loss of prime farmland[3]	—	97,666 ha	7,342 ha	13,372 ha	14,862 ha

a. Metrics presented here were quantified with the Landscape Scenario Planning Tool (LSPT), using the Marshes, Fish Support, and Agriculture analysis modules:
   1. Marsh patches are defined as contiguous regions of tidal and non-tidal emergent wetland.
   2. Large, connected wetlands are defined as wetland patches >500 ha that are contiguous with the channel network.
   3. Prime farmland grade is defined by the California Department of Conservation's Farmland Mapping and Monitoring Program's 2018 database (CDC 2018; *https://www.conservation.ca.gov/dlrp/fmmp*).

more likely to develop dendritic channel networks (Robinson et al. 2014). Increasing connectivity by decreasing the distance between marsh patches facilitates wildlife dispersal and offers rest and feeding stops for salmon and other native fish (Hammock et al. 2019; SFEI 2020). Increasing the extent of hydrologically connected marshes enhances food-web support for aquatic organisms (Cloern et al. 2021). Furthermore, restoration of tidal marsh contributes to the overall resilience of the Delta's tidal wetlands to rising sea levels (Robinson et al. 2022).

In addition to reducing GHG emissions and enhancing wildlife habitat, halting or reversing elevation losses is another critical objective for future land management in the Delta (DSC 2021b). If existing land uses are maintained, Delta organic soils may continue to subside, increasing the extent of deeply subsided land—defined as 3 m or more below sea level—by an estimated 7,500 ha (Table 4). Continued subsidence combined with rising sea levels threatens the region's infrastructure and economy; without conversion to alternative land uses, elevation losses can exacerbate strain on levees as a result of hydraulic pressures and seepage (Deverel, Bachand, et al. 2016), increasing pumping costs and the risk of catastrophic levee failures, and reducing the viability of continued farming in deeply subsided areas (Deverel et al. 2017). These risks are expected to increase into the future as SLR accelerates (Nerem et al. 2018). Additionally, we found that the extent of land at intertidal elevations is expected to decrease by 2,200 ha under *Reference*-scenario conditions, as a result of both subsidence and SLR (Table 4). This loss of intertidal land represents a loss of opportunities to restore functioning tidal wetlands that can build elevations and/or migrate upslope in response to SLR (Thorne et al. 2018).

Our scenarios demonstrate both the scale of the opportunity and the scale of the challenge for wetlands to mitigate future elevation losses. In the four future restoration and rice conversion scenarios, modeled land surface elevations in restored wetlands were estimated as much as 2 m higher than the *Reference* scenario after 40 years. We found that widespread conversion to wetlands in the *Maximum Potential* scenario built elevations Delta-wide, which reduced the extent of deeply subsided land by over 20,000 ha relative to the *Reference* scenario and roughly doubled the land area at intertidal elevations (Table 4). The degree of subsidence mitigation the other three

https://doi.org/10.15447/sfews.2024v22iss2art3

scenarios provided varied with the acreages of new wetland types. Of these three scenarios, we found that *GHG 1* provided the greatest reduction in the extent of deeply subsided land, whereas *GHG-habitat* reduced elevation losses at intertidal elevations. These effects could protect the Delta's levee system in meaningful ways. Deverel, Bachand, et al. (2016) found that growing rice or wetlands adjacent to 190 km of the levees at greatest risk could decrease the failure rate by 50%. With all three scenarios, however, we predicted an increase in deeply subsided land and loss of land at or above intertidal elevations as a result of SLR and ongoing subsidence in non-wetted sites, highlighting the challenge faced by Delta land and water managers.

Comparing the GHG, habitat, and elevation benefits of the alternative future scenarios highlights trade-offs and synergies between different management objectives. Given their sole focus on GHG benefits, *GHG 1* and *GHG 2* provided the highest absolute and per-area rate of GHG emissions reductions (Figure 4). Because GHG emissions in the *Reference* scenario were tightly linked to subsidence, these two scenarios also maximized per-area subsidence mitigation. In contrast, the *GHG-Habitat* scenario incorporates two divergent objectives: restoring intertidal habitat and reducing subsidence and associated GHG emissions. Compared with *GHG 1* and *GHG 2*, *GHG-Habitat* offers the lowest per-area rate of GHG emissions reductions because of both the inclusion of tidal wetland and the stipulation that 3,500 acres (1,400 ha) of non-tidal peat-building wetland be placed at shallow sub-tidal elevations (elevations with lower *Reference*-scenario rates of subsidence or GHG emissions; Table 1). This focus on intertidal restoration, while less beneficial for decreasing GHG emissions, supports a range of habitat functions, particularly wetland-channel connectivity that is important for fish and other aquatic organisms (Table 6; Hammock et al. 2019; SFEI 2020; Cloern et al. 2021). Additionally, restoration at both intertidal and shallow sub-tidal elevations mitigates losses of intertidal land from SLR (Table 4).

Whereas this study focused on the effects of sustained agriculture, conversion to rice, and expansion of perennial wetlands, future conditions may include other land-cover changes as a result of management or climate effects, such as levee breaches and permanent flooding of islands for water supply or fish-rearing habitat. Such future changes would alter business-as-usual conditions and influence opportunities for wetland-based subsidence and GHG mitigation. Similarly, SLR will likely lead to a loss over time of opportunities for tidal wetland restoration. The extent of wetlands at intertidal elevations will likely decline over time with SLR, particularly where hard infrastructure or other development limits the ability for intertidal zones to migrate upslope (Heady et al. 2018; Thorne et al. 2018; Robinson et al. 2022). In shallowly subsided areas, it will likely become increasingly challenging for peat-building wetlands to reach intertidal elevations needed for tidal reconnection. These effects are expected to accelerate later in the century as a result of increasing SLR rates (Nerem et al. 2018).

Addressing Economic Challenges of Land-Use Conversion

There is a growing recognition among land-owners in the Delta that subsidence mitigation is urgently needed to protect vulnerable levees and maintain arability (Deverel et al. 2015; Deverel, Bachand, et al. 2016). However, implementing proposed land-use changes for subsidence mitigation presents financial challenges. Because the majority of the deeply subsided central Delta is in private ownership, it would be beneficial in the near term to identify and implement changes that can continue to provide reasonable income and support ongoing levee maintenance, thus supporting water-supply reliability. One such change is conversion of drained agriculture to rice. Rice cultivation provides sustained farm income while halting subsidence by maintaining saturated soils for much of the year (Hatala et al. 2012; Knox et al. 2015; Deveral, Ingrum, et al 2016; Deverel et al. 2017; Whipple et al. 2022), thus providing a subsidence-mitigation strategy that also helps continue the Delta's agricultural heritage in support of the coequal goals (DSC

2013). Additionally, although rice cultivation is a net source of GHG emissions because of CH_4 production (Table 5), strategic placement of rice in the most rapidly subsiding areas can provide a net GHG and carbon benefit relative to baseline (*Reference*-scenario) emissions.

Non-tidal peat-building wetlands can also provide income in the voluntary carbon market (Deverel et al. 2017). In the near term, however, current carbon prices are not high enough to cover lost agricultural income and the large initial capital cost associated with wetland construction. For an estimated present-day carbon price of $10 per t on the voluntary market, converting rapidly subsiding land to impounded wetland could generate roughly $300 per ha annually from the sale of carbon offsets. (This estimate is based on rice and managed wetland in the *GHG-Habitat* scenario, assuming a risk score of 14% and 10% uncertainty; ACR 2017). If California's cap-and-trade program allows carbon credits from Delta wetlands to be sold on the compliance market, the carbon price is expected to double (based on past sale prices and expert opinion), and future carbon offset prices may rise substantially higher. The World Bank (2022) reported record carbon offset prices in the European Union, California, New Zealand, and the Republic of Korea, among other markets, with price increases driven by a combination of policy reforms, anticipated increased procurement of carbon offsets, speculative investment interest, changes in supply of marketable credits, and broader economic trends, especially in global energy commodity markets. Global carbon pricing revenue increased by almost 60% in the past year, and markets are growing rapidly (World Bank 2022). These economic trends indicate the potential in the Delta for carbon offsets to facilitate wetland conversion.

In addition to rice production and the sale of carbon credits, paludiculture (Joosten et al. 2016) is another potential source of wetland-based income for land-owners in the Delta. A growing technical literature points to widespread recognition of the benefits of allowing previously drained wetlands to be re-flooded and maintained for biomass production and harvest (e.g., Joosten et al. 2016). Small-scale paludiculture projects are occurring in Southeast Asia, Canada, Germany, Poland, and elsewhere throughout the European Union, with sites including rewetted peatlands. One end use of paludiculture production is the sale of biomass for alternative fuels and bio-products such as building materials. The available information (Mshandete 2009; Suda et al. 2009) indicates that periodic harvest of Delta wetland biomass could be used to generate biofuels, which would provide revenue through the use of the state's Low Carbon Fuel Standard (LCFS) incentive that provides income to producers of low-carbon fuels.

Subsidence mitigation requires near-term and long-term solutions. In the near term, creating a land-use mosaic that includes wetland agriculture on soils with high organic matter and other traditional crops in lower organic-matter soils (Whipple et al. 2022) provides a potential path forward. This mosaic would provide sustained agricultural revenues, which can finance near-term subsidence mitigation through impounded wetlands in high-priority, deeply subsided areas. Over the longer term, projected increases in carbon market revenue and the financial benefits of reducing the probability of future levee failure may be sufficient to incentivize a larger-scale conversion to non-tidal peat-building wetlands and tidal wetlands.

CONCLUSIONS

Land-use conversions in the Delta that increase the extent of saturated soils have the potential to support the coequal goals in multiple ways. By reducing oxidation and building peat stocks, conversion of drained sites to rice, impounded, or tidal wetland can limit subsidence, build elevations, and create a future Delta that is more resilient to SLR. In subsided areas, converting drained land uses to rice or non-tidal peat-building wetland can buffer levees against increased strain and seepage from rising sea levels while protecting and increasing carbon stocks in the Delta's organic soils. Such land-

https://doi.org/10.15447/sfews.2024v22iss2art3

use conversions maintain high rates of CO_2 uptake while reducing ongoing oxidation—substantially reducing GHG emissions by as much as ~80 t CO_2e ha^{-1} yr^{-1} in the most rapidly subsiding areas. Tidal wetland restoration in the Delta supports ecological functions important for wildlife. These functions include increasing habitat connectivity needed by juvenile salmonids (SFEI 2020), improving foraging success by Delta Smelt and other fish that forage in tidal channels (Howe et al. 2014; Hammock et al. 2019), providing food and nesting habitat for migratory birds and waterfowl (Spautz et al. 2005), and increasing primary production inputs to the aquatic food web (Cloern et al. 2021).

The scenarios we evaluated represent a very different landscape from the Delta of today. Achieving wetland restoration at this scale—and at a pace that could meet climate change mitigation and resilience targets—presents a considerable challenge, given the region's complex interests and current land uses. This study highlights the potential for multiple benefits from wetland restoration and rice but is not a roadmap to implementation. Rather, this study lays the groundwork for finer-scale project planning analyses that can capture on-the-ground ecological, engineering, and economic realities. In particular, trade-offs and synergies among restoration benefits demonstrate the importance of having clear objectives for multiple landscape functions when developing and evaluating land-use plans and targets.

Given the complex management goals, interests, and opportunities in the Delta, balancing these priorities presents a considerable challenge for landowners, government agencies, and other land-use planners. A strategic land-management portfolio that includes rice cultivation and both tidal and non-tidal peat-building wetlands can be designed to maximize a broad suite of benefits for ecosystems and people, addressing the diverse needs of Delta stakeholders and supporting the coequal goals. Such a strategic portfolio should include both near-term and longer-term strategies to address the pressing risks of subsidence and SLR while creating a sustainable land-use mosaic that supports functioning Delta ecosystems for decades into the future. In the near term, inclusion of rice in future land-use mosaics can halt subsidence, help stabilize levees and reduce maintenance costs, and substantially reduce GHG emissions—while providing agricultural income to offset the costs of wetland creation and restoration. Over the longer term, identifying economically viable ways to increase wetland habitat can provide sustained carbon sequestration and elevation benefits, GHG emissions reductions, and vital habitat for the Delta's fish, bird, and other wildlife populations.

This study's 40-year modeling time-frame addresses a near-term future for which we can make reasonable assumptions about SLR rates, levee infrastructure, and other factors related to climate change and management decisions. Later this century and beyond, the effects of climate change are challenging to predict, but are broadly expected to intensify pressures on Delta agriculture, water-supply reliability, and ecosystems as a result of SLR, fluvial flooding, drought, and extreme heat. Such challenges include levee seepage and flooding in agricultural lands, increasing water temperatures in channel and wetland habitats, and loss of tidal wetland from rising sea levels (DSC 2021b). As subsidence and SLR progress, the Delta may experience not only increasing climate change vulnerability and effects, but also a potential loss of opportunities to restore wetland habitat and implement changes that could maintain a productive agricultural economy. The earlier action is taken to mitigate subsidence, restore ecosystems, and reduce ongoing GHG emissions from Delta soils, the greater the opportunities for a resilient Delta ecosystem, economy, and water supply—and the greater the Delta's contributions to California's climate change mitigation goals.

ACKNOWLEDGEMENTS

Support for this work was generously provided by the California Department of Fish and Wildlife through the Proposition 1 Delta Water Quality and Ecosystem Restoration Grant Program. We are grateful to our expert advisors for providing

guidance on project design and interpretation: Campbell Ingram, Dennis Baldocchi, Ariane Arias–Ortiz, Lisa Schile–Beers, Patty Oikawa, David Schoellhamer, Kevin Buffington, Steve Crooks, and Dylan Chapple. We also thank Daphne Szutu, Gwen Miller, Ruth Askevold, and Kyle Stark for their assistance with data compilation and manuscript preparation. Any use of trade, firm, or product names is for descriptive purposes only and does not imply endorsement by the US Government.

REFERENCES

[AB 1279, Muratsuchi] 2021. [2021-2022 Regular Session.] (Cal. 2021). The California Climate Crisis Act. [accessed 2024 May 25]. Available from: *https://legiscan.com/CA/text/AB1279/id/2604954/California-2021-AB1279-Amended.html*

[ACR] American Carbon Registry at Winrock International. 2017. Methodology for the quantification, monitoring, reporting and verification of greenhouse gas emissions reductions and removals from the restoration of California deltaic and coastal wetlands. Version 1.1. [accessed 2022 Apr 14]. Available from: *https://acrcarbon.org/methodology/restoration-of-california-deltaic-and-coastal-wetlands/*

Anthony TL, Silver WL. 2020. Mineralogical associations with soil carbon in managed wetland soils. Glob Change Biol. [accessed 2020 Aug 20];26(11) 6555–6567. *https://doi.org/10.1111/gcb.15309*

Arias–Ortiz A, Oikawa PY, Carlin J, Masqué P, Shahan J, Kanneg S, Paytan A, Baldocchi DD. 2021. Tidal and nontidal marsh restoration: a trade-off between carbon sequestration, methane emissions, and soil accretion. J Geophys Res Biogeosci. [accessed 2022 Jan 5];126(12): e2021JG006573. *https://doi.org/10.1029/2021JG006573*

Arias–Ortiz A, Wolfe J, Holmquist JR, McNicol G, Needleman B, Stuart–Haentjens EJ, Windham–Myers L, Bridgham SD, Knox S, Megonigal P, et al, 2021. A synthesis of tidal wetland methane emissions across the contiguous United States. In: *AGU Fall Meeting Abstracts*, vol. 2021, p. B21C-04. [accessed 2024 Apr 18]. Available from: *https://ui.adsabs.harvard.edu/abs/2021AGUFM.B21C..04A/abstract*

Atwater BF, Belknap DF. 1980. Tidal-wetland deposits of the Sacramento–San Joaquin Delta, California. In: Field ME, Bouma AH Colburn IP, Douglas RG, and Ingle JC. 1980. Pacific Coast Paleogeography Symposium 4: Quaternary Depositional Environments of the Pacific Coast. [unknown] (CA): © 2012 Pacific Section SEPM, Society for Sedimentary Geology. [accessed 2023 Mar 11]. Available from *https://archives.datapages.com/data/pac_sepm/028/028001/pdfs/89.htm*

Aylward CM, Barthman–Thompson L, Bean WT, Kelt DA, Sacks BN, Statham MJ. 2023. Patch size and connectivity predict remnant habitat occupancy by an endangered wetland specialist, the salt marsh harvest mouse. Landsc Ecol. [accessed 2024 Apr 18];38:2053–2067. *https://doi.org/10.1007/s10980-023-01683-1*

Bates D, Maechler M, Bolker BM, Walker S. 2014. lme4: Linear mixed-effects models using Eigen and S4. R package version 1.1–7. *http://CRAN.R-project.org/package=lme4*

Beagle J, Lowe J, McKnight K, Safran S, Tam L, Szambelan S. 2019. San Francisco Bay shoreline adaptation atlas: working with nature to plan for sea level rise using operational landscape units. Report #915. [accessed 2024 Apr 18]. Richmond (CA): San Francisco Estuary Institute and SPUR. *https://doi.org/10.13140/RG.2.2.22416.46083*

Bridgham SD, Megonigal JP, Keller JK, Bliss NB, Trettin C. 2006. The carbon balance of North American wetlands. Wetlands. [accessed 2022 Mar 11];(26):889–916. *https://doi.org/10.1672/0277-5212(2006)26[889:TCBONA]2.0.CO;2*

Callaway JC, Borgnis EL, Turner RE, Milan CS. 2012. Carbon sequestration and sediment accretion in San Francisco Bay tidal wetlands. Estuaries Coasts. [accessed 2020 Jul 15];35:1163–1181. *https://doi.org/10.1007/s12237-012-9508-9*

Callaway JC, Nyman JA, DeLaune RD. 1996. Sediment accretion in coastal wetlands: a review and a simulation model of processes. Curr Top Wetl Biogeochem. [accessed 2022 Jul 28];2:23. Available from: *researchgate.net/publication/284056250_Sediment_accretion_in_coastal_wetlands_A_review_and_a_simulation_model_of_processes*

[CARB] California Air Resources Board. 2018. An inventory of ecosystem carbon in California's natural and working lands: 2018 edition. [accessed 2022 Oct 13]. Available from: *https://ww3.arb.ca.gov/cc/inventory/pubs/nwl_inventory.pdf*

[CARB] California Air Resources Board. 2022. 2022 Scoping plan for achieving carbon neutrality. [accessed 2022 Nov 29]. Available from: *https://ww2.arb.ca.gov/our-work/programs/ab-32-climate-change-scoping-plan/2022-scoping-plan-documents*

[CDC] California Department of Conservation. 2018. Farmland Mapping and Monitoring Program: Database. [accessed 2019 Mar 29]. Available from: *https://www.conservation.ca.gov/dlrp/fmmp*

[CDFW] California Department of Fish and Wildlife. 2019. Vegetation and land use classification and map update of the Sacramento–San Joaquin River Delta. [accessed 202 Jan 30]. Available from: *https://nrm.dfg.ca.gov/FileHandler.ashx?DocumentID=174866&inline*

[CDWR and LandIQ] California Department of Water Resources, Land IQ, LLC. 2020. 2016 Statewide Crop Mapping. [accessed 2020 Sep 15]. Available from: *https://data.cnra.ca.gov/dataset/statewide-crop-mapping/resource/3b57898b-f013-487a-b472-17f54311edb5*

[CDWR and USGS] California Department of Water Resources, US Geological Survey. 2019. LiDAR Data for the Sacramento–San Joaquin Delta and Suisun Marsh. [accessed 2020 Apr 30]. Available from: *http://gisarchive.cnra.ca.gov/iso/ImageryBaseMapsLandCover/LIDAR/DeltaLIDAR2017/LiDAR%20factsheet_FINAL_June2019.pdf*

Cloern JE, Safran SM, Smith Vaughn L, Robinson A, Whipple AA, Boyer KE, Drexler JZ, Naiman RJ, Pinckney JL, Howe ER, et al. 2021. On the human appropriation of wetland primary production. Sci Total Environ. [accessed 2021 May 27];785:147097. *https://doi.org/10.1016/j.scitotenv.2021.147097*

[CNRA] California Natural Resources Agency, California Environmental Protection Agency, California Department of Food and Agriculture, California Air Resources Board, California Strategic Growth Council. 2019. Draft California 2030 Natural and Working Lands Climate Change Implementation Plan. Sacramento (CA): [accessed 2021 Dec 1]. Available from: *https://ww3.arb.ca.gov/cc/natandworkinglands/draft-nwl-ip-040419.pdf*

Colombano DD, Litvin SY, Ziegler SL, Alford SB, Baker R, Barbeau MA, Cebrián J, Connolly RM, Currin CA, Deegan LA, et al. 2021. Climate change implications for tidal marshes and food web linkages to estuarine and coastal nekton. Estuaries Coasts. [accessed 2022 Jul 21];44:1637–1648. *https://doi.org/10.1007/s12237-020-00891-1*

Craig MS, Kundariya N, Hayashi K, Srinivas A, Burnham M, Oikawa P. 2017. Geophysical surveying in the Sacramento Delta for earthquake hazard assessment and measurement of peat thickness. In: American Geophysical Union, Fall Meeting 2017, abstract #T23G-07. [accessed 2024 Apr 18];T23G-07. Available from: *https://ui.adsabs.harvard.edu/abs/2017AGUFM.T23G..07C/abstract*

De Gryze S, Wolf A, Kaffka SR, Mitchell J, Rolston DE, Temple SR, Lee J, Six J. 2010. Simulating greenhouse gas budgets of four California cropping systems under conventional and alternative management. Ecol Appl. [accessed 2022 Apr 28];20:1805–1819. *https://doi.org/10.1890/09-0772.1*

Deverel SJ, Bachand S, Brandenberg SJ, Jones CE, Stewart JP, Zimmaro P. 2016. Factors and processes affecting delta levee system vulnerability. San Franc Estuary Watershed Sci. [accessed 2019 Nov 08];14(4). [accessed 2019 Nov 8]. *https://escholarship.org/uc/item/36t9s0mp*

Deverel SJ, Dore S, Schmutte C. 2020. Solutions for subsidence in the California Delta, USA, an extreme example of organic-soil drainage gone awry. Proc Int Assoc Hydrol Sci. [accessed 2022 Jul 28];382:837–842. *https://doi.org/10.5194/piahs-382-837-2020*

Deverel SJ, Ingrum T, Leighton D. 2016. Present-day oxidative subsidence of organic soils and mitigation in the Sacramento–San Joaquin Delta, California, USA. Hydrogeol J. [accessed 2020 Aug 18];24:569–586. *https://doi.org/10.1007/s10040-016-1391-1*

Deverel S, Ingrum T, Lucero C, Hydrofocus, Inc., Drexler J, US Geological Survey. 2014. Impounded marshes on subsided islands: simulated vertical accretion, processes, and effects, Sacramento–San Joaquin Delta, CA USA. San Franc Estuary Watershed Sci. [accessed 2019 Nov 08];12(2). *https://doi.org/10.15447/sfews.2014v12iss2art5*

Deverel S, Jacobs P, Lucero C, Dore S, Kelsey TR. 2017. Implications for greenhouse gas emission reductions and economics of a changing agricultural mosaic in the Sacramento–San Joaquin Delta. San Franc Estuary Watershed Sci. [accessed 2021 Sep 20];15(3). *https://doi.org/10.15447/sfews.2017v15iss3art2*

Deverel S, Leighton DA. 2010. Historic, recent, and future subsidence, Sacramento–San Joaquin Delta, California, USA. San Franc Estuary Watershed Sci. [accessed 2019 Nov 12];8(2). *https://doi.org/10.15447/sfews.2010v8iss2art1*

Deverel SJ, Lucero CE, Bachand S. 2015. Evolution of arability and land use, Sacramento–San Joaquin Delta, California. San Franc Estuary Watershed Sci. [accessed 2020 Jun 18];13(2). *https://doi.org/10.15447/sfews.2015v13iss2art4*

Deverel SJ, Rojstaczer S. 1996. Subsidence of agricultural lands in the Sacramento–San Joaquin Delta, California: role of aqueous and gaseous carbon fluxes. Water Resour Res. [accessed 2022 Jul 25];32:2359–2367. *https://doi.org/10.1029/96WR01338*

Dong H, Mangino J, McAllister TA, Hatfield JL, Johnson DE, Lassey KR, Aparecida d Lima M, Romanovskaya A. 2006. Emissions from livestock and manure management. Volume 4: Agricultural, forestry and other land use. Chapter 10 in: IPCC Guidelines for National Greenhouse Gas Inventories. [accessed 2022 Apr 28]. Geneva (Switzerland): IPCC. Available from: *https://www.ipcc-nggip.iges.or.jp/public/2006gl/vol4.html*

Drexler JZ, de Fontaine CS, Brown TA. 2009. Peat accretion histories during the past 6,000 years in marshes of the Sacramento–San Joaquin Delta, CA, USA. Estuaries Coasts Port Repub. [accessed 2022 Mar 11];32:871–892. *https://doi.org/10.1007/s12237-009-9202-8*

Drexler JZ, de Fontaine CS, Deverel SJ. 2009. The legacy of wetland drainage on the remaining peat in the Sacramento–San Joaquin Delta, California, USA. Wetlands. [accessed 2022 Mar 11];29:372–386. *https://doi.org/10.1672/08-97.1*

Drexler JZ, Khanna S, Lacy JR. 2021. Carbon storage and sediment trapping by *Egeria densa* Planch., a globally invasive, freshwater macrophyte. Sci Total Environ. [accessed 2024 Apr 18];755:142602. *https://doi.org/10.1016/j.scitotenv.2020.142602*

Drexler JZ, Khanna S, Schoellhamer DH, Orlando J. 2019. The fate of blue carbon in the Sacramento–San Joaquin Delta of California, USA. In: Windham-Myers L, Crooks S, Troxler TG, editors. A blue carbon primer: the state of coastal wetland carbon science, practice and policy. Boca Raton (FL): CRC Press. p. 307–325.

[DSC] Delta Stewardship Council. 2013. The Delta plan — ensuring a reliable water supply for California, a healthy Delta ecosystem and a place of enduring value. [accessed 2022 Jun 28]. Available from: *https://deltacouncil.ca.gov/delta-plan/*

[DSC] Delta Stewardship Council. 2022a. Protect, restore, and enhance the Delta ecosystem. [accessed 2022 Jul 21]. Chapter 4 in: Delta plan. Amended June 2022. Available from: *https://deltacouncil.ca.gov/pdf/delta-plan/2022-06-29-chapter-4-protect-restore-and-enhance-the-delta-ecosystem.pdf*

[DSC] Delta Stewardship Council. 2022b. Methods used to update ecosystem restoration maps using new digital elevation model and tidal data. Appendix Q1 in: Delta Plan Amendments. [accessed 2022 Jul 21]. Available from: *https://deltacouncil.ca.gov/pdf/delta-plan/2022-06-29-appendix-q1-methods-used-to-update-ecosystem-restoration-maps-using-new-digital-elevation-model-and-tidal-data.pdf*

[DSC] Delta Stewardship Council. 2021a. Delta adapts: creating a climate resilient future. Technical Memorandum, Flood Hazard Assessment, June 2021. [accessed 2022 Jun 29]. Sacramento (CA): Delta Stewardship Council. Available from: *https://www.deltacouncil.ca.gov/pdf/delta-plan/2021-06-17-flood-hazard-assessment-technical-memorandum.pdf*

[DSC] Delta Stewardship Council. 2021b. Delta adapts: creating a climate resilient future. [website]. [accessed 2022 Jun 29]. Available from: *https://deltacouncil.ca.gov/delta-plan/climate-change*

Durand JR. 2015. A conceptual model of the aquatic food web of the upper San Francisco Estuary. San Franc Estuary Watershed Sci. [accessed 2022 Jul 21];13(3). *https://doi.org/10.15447/sfews.2015v13iss3art5*

Dybala K, Gardali T, Melcer J. 2020. Getting our heads above water: integrating bird conservation in planning, science, and restoration for a more resilient Sacramento–San Joaquin Delta. San Franc Estuary Watershed Sci. [accessed 2022 Apr 26];18(4). *https://doi.org/10.15447/sfews.2020v18iss4art2*

Hammock BG, Hartman R, Slater SB, Hennessy A, Teh SJ. 2019. Tidal wetlands associated with foraging success of Delta Smelt. Estuaries Coasts. [accessed 2022 Jul 26];42:857–867. *https://doi.org/10.1007/s12237-019-00521-5*

Hatala JA, Detto M, Sonnentag O, Deverel SJ, Verfaillie J, Baldocchi DD. 2012. Greenhouse gas (CO_2, CH_4, H_2O) fluxes from drained and flooded agricultural peatlands in the Sacramento–San Joaquin Delta. Agric Ecosyst Environ. [accessed 2022 Jan 13];150:1–18. *https://doi.org/10.1016/j.agee.2012.01.009*

Heady WN, Cohen BS, Gleason MG, Morris JN, Newkirk SG, Klausmeyer KR, Walecka HR, Gagneron E, Small M. 2018. Conserving California's coastal habitats: a legacy and a future with sea level rise. [accessed 2022 May 31]. San Francisco (CA): The Nature Conservancy; Oakland (CA): California State Coastal Conservancy. Available from: *https://www.scienceforconservation.org/products/coastal-assessment*

Hemes KS, Chamberlain SD, Eichelmann E, Anthony T, Valach A, Kasak K, Szutu D, Verfaillie J, Silver WL, Baldocchi DD. 2019. Assessing the carbon and climate benefit of restoring degraded agricultural peat soils to managed wetlands. Agric For Meteorol. [accessed 202 May 11];268:202–214. *https://doi.org/10.1016/j.agrformet.2019.01.017*

Howe ER, Simenstad CA, Toft JD, Cordell JR, Bollens SM. 2014. Macroinvertebrate prey availability and fish diet selectivity in relation to environmental variables in natural and restoring north San Francisco Bay tidal marsh channels. San Franc Estuary Watershed Sci. [accessed 2022 Jul 21];12(1). *https://doi.org/10.15447/sfews.2014v12iss1art5*

Ingebritsen SE, Ikehara ME, Galloway DL, Jones DR. 2000. Delta subsidence in California: the sinking heart of the state. [accessed 2022 Sep 26]. Reston (VA): US Geological Survey. Fact Sheet 005-00. *https://doi.org/10.3133/fs00500*

Joosten H, Gaudig G, Tanneberger F, Wichmann S, Wichtmann W. 2016. Paludiculture: sustainable productive use of wet and rewetted peatlands. In: Bonn A, et al., editors. 2016. Peatland restoration and ecosystem services science, policy and practice. Cambridge (UK): Cambridge University Press. p 339–357.

Knox AK, Dahlgren RA, Tate KW, Atwill ER. 2008. Efficacy of natural wetlands to retain nutrient, sediment and microbial pollutants. J Environ Qual. [accessed 2024 Apr 28];37:1837–1846. *https://doi.org/10.2134/jeq2007.0067*

Knox SH, Sturtevant C, Matthes JH, Koteen L, Verfaillie J, Baldocchi D. 2015. Agricultural peatland restoration: effects of land-use change on greenhouse gas (CO_2 and CH_4) fluxes in the Sacramento–San Joaquin Delta. Glob Change Biol. [accessed 202 Aug 18];21:750–765. *https://doi.org/10.1111/gcb.12745*

Kroodsma DA, Field CB. 2006. Carbon sequestration in California agriculture, 1980–2000. Ecol Appl. [accessed 2022 Jan 25];16:1975–1985. *https://doi.org/10.1890/1051-0761(2006)016[1975:CSICA]2.0.CO;2*

Kuznetsova A, Brockhoff PB, Christensen RHB. 2014. lmerTest: tests for random and fixed effects for linear mixed effect models (lmer objects of lme4 package). R package version 2.0-11. Available from: *http://CRAN.R-project.org/package=lmerTest*

Ma S, Baldocchi DD, Xu L, Hehn T. 2007. Inter-annual variability in carbon dioxide exchange of an oak/grass savanna and open grassland in California. Agric For Meteorol. [accessed 2021 Feb 16];147:157–171. *https://doi.org/10.1016/j.agrformet.2007.07.008*

Miller RL, Fram M, Fujii R, Wheeler G. 2008. Subsidence reversal in a re-established wetland in the Sacramento–San Joaquin Delta, California, USA. San Franc Estuary Watershed Sci. [accessed 2021 May 12];6(3). *https://doi.org/10.15447/sfews.2008v6iss3art1*

Morris JT, Barber DC, Callaway JC, Chambers R, Hagen SC, Hopkinson CS, Johnson BJ, Megonigal P, Neubauer SC, Troxler T, et al. 2016. Contributions of organic and inorganic matter to sediment volume and accretion in tidal wetlands at steady state. Earths Future. [accessed 2021 Sep 22];4:110–121. *https://doi.org/10.1002/2015EF000334*

Morris JT, Bowden WB. 1986. A mechanistic, numerical model of sedimentation, mineralization, and decomposition for marsh sediments. Soil Sci Soc Am J. [accessed 2021 Oct 15];50:96. *https://doi.org/10.2136/sssaj1986.03615995005000010019x*

Morris JT, Cahoon D, Callaway JC, Craft C, Neubauer SC, Weston NB. 2021. Marsh equilibrium theory: implications for responses to rising sea level. In: FitzGerald D, Hughes Z, editors. Salt marshes: function, dynamics, and stresses. Cambridge (UK): Cambridge University Press. p. 157–177. Available from: *https://www.cambridge.org/core/books/abs/salt-marshes/marsh-equilibrium-theory/DA7B5EFE9C8CE403EF2190CC60D968EF*

Morris JT, Drexler J, Vaughn LS, Robinson A. 2022. An assessment of future tidal marsh resilience in the San Francisco Estuary through modeling and quantifiable metrics of sustainability. Front Environ Sci. [accessed 2022 Jul 22];10. *https://doi.org/10.3389/fenvs.2022.1039143*

Morris JT, Edwards J, Crooks S, Reyes E. 2012. Assessment of carbon sequestration potential in coastal wetlands. In: Lal R, Lorenz K, Hüttl RF, Schneider BU, von Braun J, editors. Recarbonization of the biosphere: ecosystems and the global carbon cycle. [accessed 2022 Nov 30]. Dordrecht (Netherlands): Springer. p. 517–531. *https://doi.org/10.1007/978-94-007-4159-1_24*

Morris JT, Renken KA. 2020. Past, present, and future nuisance flooding on the Charleston Peninsula. PLoS ONE. [accessed 2022 Jul 20];15:e0238770. *https://doi.org/10.1371/journal.pone.0238770*

Mount J, Twiss R. 2005. Subsidence, sea level rise, and seismicity in the Sacramento–San Joaquin Delta. San Franc Estuary Watershed Sci. [accessed 2021 Sep 27];3(1). *https://doi.org/10.15447/sfews.2005v3iss1art7*

Mshandete AM. 2009. The Anaerobic digestion of cattail weeds to produce methane using American cockroach gut microorganisms. ARPN J Agric Biol Sci. [accessed 2022 Jul 28];4:1–13. Available from: *https://www.researchgate.net/publication/239592731_The_anaerobic_digestion_of_cattail_weeds_to_produce_methane_using_American_cockroach_gut_microorganisms*

Myhre G, Shindell D, Bréon F–M, Collins W, Fuglestvedt J, Huang J, Koch D, Lamarque J–F, Lee D, Mendoza B, et al. 2013. Anthropogenic and natural radiative forcing. Climate change 2013: the physical science basis. In: Stocker TF, Qin D, Plattner G–K, Tignor M, Allen SK, Boschung J, Nauels A, Xia Y, Bex V, Midgley PM, editors. Contribution of Working Group I to the Fifth Assessment Report of the Intergovernmental Panel on Climate Change. New York (NY): Cambridge University Press. p. 82.

Narayan S, Beck MW, Wilson P, Thomas CJ, Guerrero A, Shepard CC, Reguero BG, Franco G, Ingram JC, Trespalacios D. 2017. The value of coastal wetlands for flood damage reduction in the northeastern USA. Sci Rep. [accessed 2024 Apr 18];7:1–12. *https://doi.org/10.1038/s41598-017-09269-z*

Nerem RS, Beckley BD, Fasullo JT, Hamlington BD, Masters D, Mitchum GT. 2018. Climate-change-driven accelerated sea-level rise detected in the altimeter era. Proc Natl Acad Sci. [accessed 2021 Dec 17];115:2022–2025. *https://doi.org/10.1073/pnas.1717312115*

[OPC] Ocean Protection Council. 2018. State of California sea-level rise guidance: 2018 update. [accessed 2024 Apr 18]. Sacramento (CA): OPC. Available from: *https://opc.ca.gov/webmaster/ftp/pdf/agenda_items/20180314/Item3_Exhibit-A_OPC_SLR_Guidance-rd3.pdf*

Perry R, Skalski J, Brandes P, Sandstrom P, Klimley A, Ammann A, Macfarlane R. 2010. Estimating survival and migration route probabilities of juvenile Chinook Salmon in the Sacramento–San Joaquin River Delta. North Am J Fish Manag. [accessed 2024 Apr 18];30:142–156. *https://doi.org/10.1577/M08-200.1*

Prokopovich NP. 1985. Subsidence of peat in California and Florida. Environ Eng Geosci. [accessed 2022 Jul 21];4:395–420. *https://doi.org/10.2113/gseegeosci.xxii.4.395*

R Core Team. 2020. A language and environment for statistical computing. Vienna (Austria): R Foundation for Statistical Computing. Available from: *https://www.R-project.org/*

Robinson A, Harris K, Morris J, Drexler JZ, Vaughn LS, Safran S, Panlasigui S, Grenier JL, Ball D. 2022. Delta wetland futures: tidal marsh resilience to sea level rise. SFEI Contribution No. 1106. [accessed 2024 Apr 18]. Richmond (CA): San Francisco Estuary Institute. Available from: *https://www.sfei.org/documents/delta-wetland-futures-tidal-marsh-resilience-sea-level-rise*

Robinson AH, Safran SM, Beagle J, Grossinger RM, Grenier JL, Askevold RA. 2014. A Delta transformed: ecological functions, spatial metrics, and landscape change in the Sacramento–San Joaquin Delta. Resilient Landscapes Program Publication #729. [accessed 2022 Jun 28]. Richmond (CA): San Francisco Estuary Institute–Aquatic Science Center. Available from: *http://sfei.org/projects/delta-landscapes-project*

Rouleau T, Colgan CS, Adkins J, Castelletto A, Dirlam P, Lyons S, Stevens H. 2021. The economic value of America's estuaries: 2021 update. [accessed 2024 Apr 18]. Washington (DC): Restore America's Estuaries. Available from: *http://www.estuaries.org/economics/2021-report*

Safran S. 2014. Natural flow hydrodynamic modeling technology support phase 1. Technical memorandum. [accessed 2024 Jun 7]. Prepared for the Metropolitan Water District of Southern California. Richmond (CA): San Francisco Estuary Institute. 40 p. Available from: *https://www.sfei.org/documents/natural-flow-hydrodynamic-modeling-technology-support-phase-1-technical-memorandum*

[SFEI] San Francisco Estuary Institute. 2022. Landscape Scenario Planning Tool User Guide v. 2.0. [accessed 2024 Apr 18]. Richmond (CA): San Francisco Estuary Institute–Aquatic Science Center. Available from: *https://www.sfei.org/documents/landscape-scenario-planning-tool-user-guide-v20*

[SFEI] San Francisco Estuary Institute. 2020. Identifying suitable rearing habitat for Chinook Salmon in the Sacramento–San Joaquin Delta. Publication #972. Richmond (CA): San Francisco Estuary Institute–Aquatic Science Center. [accessed 2024 Apr 04]. Available from: *https://www.baydeltalive.com/assets/05058ccde7595f531c3f6b5eda7faa2f/application/pdf/DeltaSalmon_Rearing_Habitat_Final_Report_02_21_20.pdf*

Shapiro K, Conrad PA, Mazet JAK, Wallender WW, Miller WA, Largier JL. 2010. Effect of estuarine wetland degradation on transport of *Toxoplasma gondii:* surrogates from land to sea. Appl Environ Microbiol. [accessed 2024 Apr 18];76:6821–6828. *https://doi.org/10.1128/AEM.01435-10*

Signor D, Cerri CEP. 2013. Nitrous oxide emissions in agricultural soils: a review. Pesqui Agropecuária Trop. [accessed 2022 Jul 1];43:322–338. *https://doi.org/10.1590/S1983-40632013000300014*

Sommer T, Armor C, Baxter R, Breuer R, Brown L, Chotkowski M, Culberson S, Feyrer F, Gingras M, Herbold B, et al. 2007. The collapse of pelagic fishes in the upper San Francisco Estuary: El colapso de los peces pelagicos en la cabecera del Estuario San Francisco. Fisheries. [accessed 2022 Jul 21];32:270–277. *https://doi.org/10.1577/1548-8446(2007)32[270:TCOPFI]2.0.CO;2*

Spautz H, Nur N, Stralberg D. 2005. California Black Rail (*Laterallus jamaicensis coturniculus*) distribution and abundance in relation to habitat and landscape features in the San Francisco Bay. [accessed 2024 Apr 18]. In: Ralph CJ, Rich TD, editors. Bird conservation implementation and integration in the Americas. Proceedings of the 3rd International Partners in Flight Conference, March 20–24, 2002, Asilomar. US Department of Agriculture, Forest Service. 672 p. Available from: *https://www.fs.usda.gov/research/treesearch/31850*

Stralberg D, Cameron DR, Reynolds MD, Hickey CM, Klausmeyer K, Busby SM, Stenzel LE, Shuford WD, Page GW. 2011. Identifying habitat conservation priorities and gaps for migratory shorebirds and waterfowl in California. Biodivers Conserv. [accessed 2022 Jul 21];20:19–40. *https://doi.org/10.1007/s10531-010-9943-5*

Suda K, Shahbazi A, Li Y. 2009. The feasibility of using cattails from constructed wetlands to produce bioethanol. Proceedings of the 2007 National Conference on Environmental Science and Technology. Springer. pp 9-15. [accessed 2022 Jul 28];9–15. *https://doi.org/10.1007/978-0-387-88483-7_2*

Takekawa JY, Woo I, Spautz H, Nur N, Grenier JL, Malamud–Roam K, Nordby JC, Cohen AN, Malamud–Roam F, Wainwright–De La Cruz SEW. 2006. Environmental threats to tidal-marsh vertebrates of the San Francisco Bay estuary. Stud Avian Biol. [accessed 2024 Apr 18];32:176–197. Available from: *https://sora.unm.edu/sites/default/files/journals/sab/sab_032.pdf*

Teh YA, Silver WL, Sonnentag O, Detto M, Kelly M, Baldocchi DD. 2011. Large greenhouse gas emissions from a temperate peatland pasture. Ecosystems. [accessed 2022 Mar 11];14:311–325. *https://doi.org/10.1007/s10021-011-9411-4*

Thorne K, MacDonald G, Guntenspergen G, Ambrose R, Buffington K, Dugger B, Freeman C, Janousek C, Brown L, Rosencranz J, et al. 2018. US Pacific coastal wetland resilience and vulnerability to sea-level rise. Sci Adv. [accessed 2022 Mar 11];4:eaao3270. *https://doi.org/10.1126/sciadv.aao3270*

Verhoeven E, Pereira E, Decock C, Garland G, Kennedy T, Suddick E, Horwath W, Six J. 2017. N2O emissions from California farmlands: a review. Calif Agric. [accessed 2022 Feb 3];71:148–159. *https://doi.org/10.3733/ca.2017a0026*

[USEPA] United States Environmental Protection Agency 2021. Inventory of US greenhouse gas emissions and sinks, 1990–2019. [accessed 2024 Apr 18]. Washington (DC): US Environmental Protection Agency. EPA Publication #430-R-21-005. Available from: *https://www.epa.gov/sites/default/files/2021-04/documents/us-ghg-inventory-2021-main-text.pdf*

[USEPA] United States Environmental Protection Agency. 2022. Greenhouse gas equivalencies calculator. Updated March 2022. [accessed 2024 Apr 18]. Washington (DC): US Environmental Protection Agency. Available from: *https://www.epa.gov/energy/greenhouse-gas-equivalencies-calculator*

Whipple A, Grossinger RM, Rankin D, Stanford B, Askevold RA. 2012. Sacramento–San Joaquin Delta historical ecology investigation: exploring pattern and process. [accessed 202 Jun 11]. SFEI Contribution No. 672. Richmond (CA): San Francisco Estuary Institute. Available from: *https://www.sfei.org/documents/sacramento-san-joaquin-delta-historical-ecology-investigation-exploring-pattern-and-proces*

Whipple AA, Safran SM, Zeleke D, Wells E, Deverel S, Olds M, Cole S, Rodriguez–Flores J, Guzman A, Medellin–Azuara J, et al. 2022. Resilient Staten island: landscape scenario analysis pilot application. [accessed 2022 Jul 21]. Prepared for the US Fish and Wildlife Service. SFEI Resilient Landscapes Program Publication #1079. Richmond (CA): San Francisco Estuary Institute. Available from: *https://www.sfei.org/documents/resilient-staten-island-landscape-scenario-analysis-pilot-application*

Woo I, Davis MJ, De La Cruz SEW, Windham–Myers L, Drexler JZ, Byrd KB, Stuart–Haëntjens EJ, Anderson FE, Bergamaschi BA, Nakai G, et al. 2021. Carbon flux, storage, and wildlife co-benefits in a restoring estuary: case study at the Nisqually River Delta, Washington. Chapter 5 in: Wetland carbon and environmental management. American Geophysical Union. [accessed 2022 Jul 21];103–125. *https://doi.org/10.1002/9781119639305.ch5*

World Bank. 2022. State and trends of carbon pricing 2022. Washington (DC): The World Bank. [accessed 2024 Apr 18]. Available from: *https://hdl.handle.net/10986/37455*

Ye R, Espe MB, Linquist B, Parikh SJ, Doane TA, Horwath WR. 2016. A soil carbon proxy to predict CH_4 and N_2O emissions from rewetted agricultural peatlands. Agric Ecosyst Environ. [accessed 2021 Sep 20];220:64–75. *https://doi.org/10.1016/j.agee.2016.01.008*